Contrib Mineral Petrol (2000) 140: 263–282 © Springer-Verlag 2000

Ryuichi Shinjo · Jon D. Woodhead · Janet M. Hergt

Geochemical variation within the northern Ryukyu Arc: magma source compositions and geodynamic implications

Received: 30 November 1999 / Accepted: 20 July 2000

Abstract The major and trace element and Pb–Sr–Nd isotopic compositions of Quaternary mafic lavas from the northern Ryukyu arc provide insights into the nature of the mantle wedge and its tectonic evolution. Beneath the volcanic front in the northern part of the arc, the subducted slab of the Philippine Sea Plate bends sharply and steepens at a depth of ~80 km. Lavas from the volcanic front have high abundances of large ion lithophile elements and light rare earth elements relative to the high field strength elements, consistent with the result of fluid enrichment processes related to dehydration of the subducting slab. New Pb isotopic data identify two distinct asthenospheric domains in the mantle wedge beneath the south Kyushu and northern Ryukyu arc, which, in a parallel with data from the Lau Basin, appear to reflect mantle with affinities to Indian and Pacific-type mid-ocean ridge basalt (MORB). Indian Ocean MORB-type mantle, contaminated with subducted Ryukyu sediments can account for the variation of lavas erupted on south Kyushu, and probably in the middle Okinawa Trough. In contrast, magmas of the northern Ryukyu volcanic front appear to be derived from sources of Pacific MORB-type mantle contaminated with a sedimentary component. Along-arc variation in the northern Ryukyus reflects increasing involvement of a sedimentary component to the south. Compositions of alkalic basalts from the south Kyushu back-arc resemble intraplate-type basalts erupted in NW Kyushu since ~12 Ma. We propose that the bending of the subducted slab was either caused by or resulted in lateral migration of asthenospheric mantle, yielding Indian Ocean-type characteristics from a mantle upwelling zone beneath NW Kyushu and the East China Sea. This model also accounts for (1) extensional counter-clockwise crustal rotation (~4–2 Ma), (2) voluminous andesite volcanism (~2 Ma), and (3) the recent distinctive felsic magmatism in the south Kyushu region.

R. Shinjo (✉)
Department of Physics and Earth Sciences,
University of the Ryukyus, Senbaru 1,
Nishihara, Okinawa 903-0213, Japan
e-mail: rshinjo@sci.u-ryukyu.ac.jp
Tel.: +81-98-8958569; Fax: +81-98-8958552

J. D. Woodhead · J. M. Hergt
School of Earth Sciences, The University of Melbourne,
Victoria 3010, Australia

Editorial responsibility: T.L. Grove

Introduction

The Ryukyu Arc extends for a distance of ~1200 km from Kyushu, south-western Japan, to Taiwan, and has been interpreted to result from westward-dipping subduction of the Philippine Sea Plate under the Eurasian Plate (Fig. 1). In the northern arc segment, the volcanic front is defined by a number of Quaternary volcanic centres. In this region, however, there are major variations in the angle of subduction, nature of subducting slab, and style of volcanism. For example, in the north the subducting slab is characterised by a steep (70°) dip to 80 km depth at which point it bends sharply (see lower panels in Fig. 1), whereas in the southern part the slab does not bend as sharply, and dips at a shallower angle (40–50°) (e.g. Shiono et al. 1980; Nagamune 1987; Ishihara and Yoshida 1992).

There are few detailed analytical studies of the Ryukyu arc. Nakada (1986) and Tiba (1989) presented X-ray fluorescence spectrometry (XRF) of major and trace element data for volcanic rocks from selected volcanoes in the northern Ryukyu arc, and Notsu et al. (1990) reported $^{87}Sr/^{86}Sr$ ratios for a wide range of volcanic rocks from the northern Ryukyu Arc and SW Japan. More recently Arakawa et al. (1998) presented Sr–Nd isotopic and trace element data for basalts to rhyolites from the Aira Caldera in south Kyushu (Fig. 2). Although a number of Pb isotope analyses for volcanic rocks from NE and SW Japan, the Japan Sea, and eastern China have been published (e.g. Basu et al. 1991;

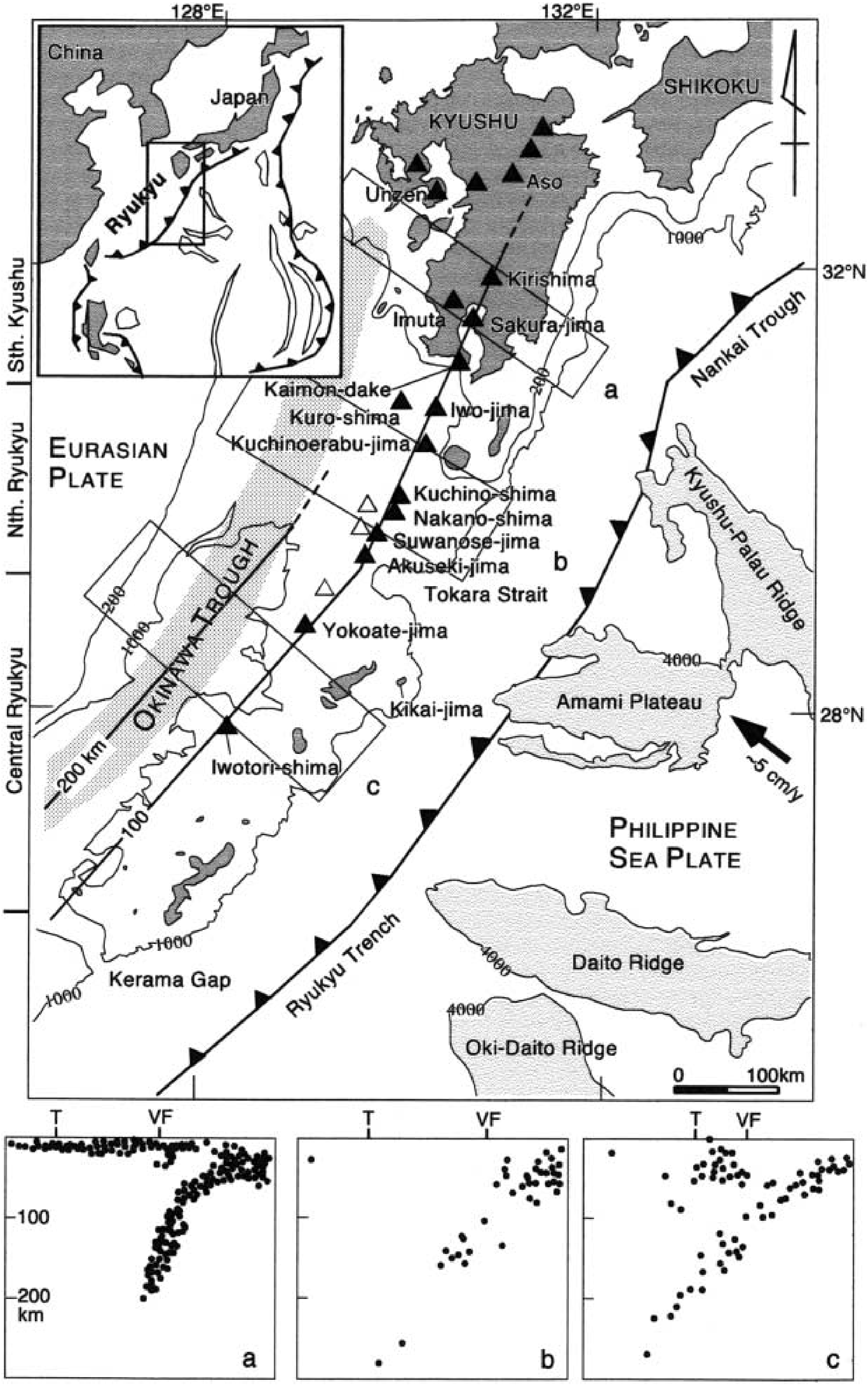

Tatsumoto and Nakamura 1991; Cousens et al. 1994; Kersting et al. 1996), such data for volcanic rocks in southern Kyushu and the northern Ryukyu arc are almost non-existent.

A number of workers have noted that the east Asian–western Pacific asthenosphere resembles Indian Ocean mid-ocean ridge basalt (MORB), particularly in terms of Pb isotopic composition (e.g. Mukasa et al. 1987; Chung

Fig. 1 Map of the northern Ryukyu arc showing the major structural elements of the convergent margin. Bathymetric contours (200 and 1000 m) are indicated. *Solid triangles*, Quaternary volcanoes; *open triangles*, M. Miocene to Pliocene volcanics. *Thick lines* represent depth contours (100 and 200 km) to the Wadati–Benioff zone (Letouzey and Kimura 1986; Ishihara and Yoshida 1992). The *solid arrow* indicates the plate motion vector of the Philippine Sea Plate relative to the Eurasian Plate (Seno et al. 1993). The island of Kikai-jima, located at 28.3°N, 130°E, is rising rapidly at a rate of 1 to 2 mm/year because of collision of the Amami Plateau with the Ryukyu Trench. Topographic highs (e.g. Amami Plateau and Daito and Oki-Daito Ridges) on the Philippine Sea Plate are outlined by a 4000-m depth contour. Lower panels show a cross section of the hypocentral distribution of earthquakes in the southern Kyushu and northern Ryukyu Arc (M. Nakamura, personal communication 2000), together with the positions of volcanic front (*VF*) and Okinawa Trough axis (*T*)

et al. 1995; Hickey-Vargas et al. 1995; Flower et al. 1998).

As a result, delineating the boundary between the Indian Ocean and Pacific MORB mantle domains and defining the extent of Indian-type mantle in eastern Asia remains an important goal for research in this region.

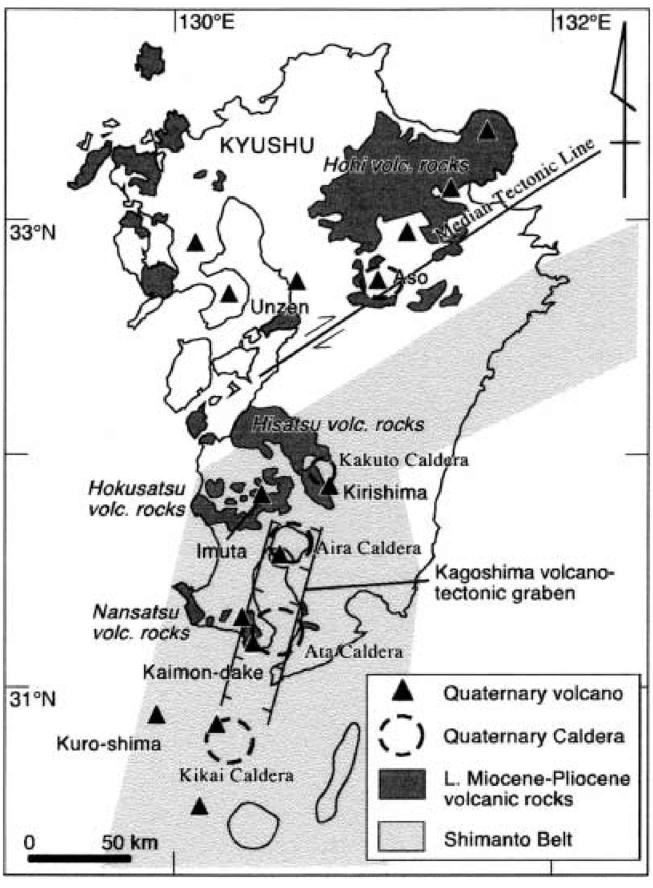

Fig. 2 Map of Kyushu Island, showing distribution of the late Cenozoic volcanic rocks. Note that late Miocene-Pliocene volcanic rocks (Hohi, Hisatsu, Hokusatsu, and Nansatsu volcanic rocks) are located behind the present volcanic front. Shimanto Belt (terrane) is also indicated

Furthermore, the tectonic variations noted above might well be expected to have some influence on the composition of the erupted magmas. Despite this, and the need to define the nature of the mantle wedge under the eastern Eurasian margin, there have been few petrological studies of Cenozoic volcanic rocks from the Ryukyu arc relative to those of NE Japan and the Japan Sea basin.

The objectives of this study are thus (1) to provide a comprehensive elemental and isotopic dataset for Quaternary basalts and basaltic andesites in the northern Ryukyu arc, (2) to identify any spatial variation in the mantle sources of mafic magma supplying this arc, and (3) to consider the geochemistry of these sources in relation to tectonic setting.

Tectonic and geological setting and samples

Arc volcanism

The Philippine Sea Plate subducts north-westwards in western Japan, forming two volcanic arcs: the Ryukyu and south-west Japan arcs. These are separated by a volcanic gap corresponding to the point where the Kyushu-Palau Ridge on the Philippine Sea Plate collides with the Eurasian Plate (Fig. 1). The Ryukyu arc has itself been divided into three segments (i.e. north, central, south Ryukyus) by the Tokara Strait (at ~29.3°N) and the Kerama Gap (~26°N), respectively; these two boundaries are considered to be left-lateral strike-slip faults (Kizaki 1986; Isozaki and Nishimura 1989).

From Kyushu Island toward the south, the Ryukyu volcanic front runs in a NNE–SSW direction, located ~100 km above the Wadati–Benioff zone (Letouzey and Kimura 1986; Ishihara and Yoshida 1992). Most of the eruptive centres along the volcanic front are currently active or have some record of historical eruptions. During the last few million years, extensive andesitic-rhyolitic volcanism also occurred on southern Kyushu itself. Some of the large eruptions produced calderas in the graben zone (the so-called Kagoshima volcano-tectonic graben) along the volcanic front (Fig. 2).

Based on K–Ar dating, Uto and Uchiumi (1997) recently proposed the presence of a second volcanic chain on the back-arc side of southern Kyushu, which includes a rhyolite volcano (Imuta) and basaltic monogenetic cinder cones. Kuro-shima, located in the back-arc region of the northern segment of north Ryukyu, is a relatively old volcano, where a K–Ar age of 1.03 ± 0.13 Ma has been reported (Joshima et al. 1978). Thus volcanoes extend ~50 km westward from the volcanic front in southern Kyushu, but volcanism becomes restricted to the volcanic front forming a single volcanic island chain (also known as the Tokara volcanic islands chain) in the northern to central Ryukyus.

A recent integration of K–Ar dates for the region revealed that the principal locus of volcanic activity in south Kyushu has migrated eastward with time since

~4 Ma (Fig. 2; Watanabe et al. 1993; Uto et al. 1997). In the northern Ryukyu arc, volcanism also shifted to the east after the Pliocene, giving rise to a double row of islands (Fig. 1; e.g. Daishi et al. 1987). This trench-ward migration of volcanism may imply steepening of the dip of the Wadati–Benioff zone accompanying trench rollback.

Ocean-island basalt (OIB)-like volcanism

In north-western Kyushu, basalts have been emplaced from ~12 Ma to present (Fig. 2; Nakamura et al. 1990; Nakada and Kamata 1991). However, because seismic data indicate that the subducted Philippine Sea Plate is not present under NW Kyushu (Fig. 1), it is possible that this activity was not directly related to subduction. Most of the erupted lavas are Miocene in age, and formed extensive lava plateaus, although some modern shield volcanoes are also observed. Incompatible element patterns of these NW Kyushu basalts are typical of those for ocean-island basalt (OIB; Nakamura et al. 1985, 1990; Nakada and Kamata 1991).

Tectonic setting and subduction of the Philippine Sea Plate

Subduction of the Philippine Sea Plate to the north began in the latest Miocene (Yamamoto 1993). Evidence from the nature of volcanism in SW Japan suggests a hiatus or slowing of subduction during the period 10–6 Ma (Kamata and Kodama 1994), but convergence is now occurring in the northern Ryukyu arc at a rate of ~5 cm/year relative to the Eurasian Plate in the direction of ˜305° (Fig. 1; Seno et al. 1993).

As noted by several authors (e.g. Nagamune 1987; Ishihara and Yoshida 1992), there is a major change in the character of the Wadati–Benioff zone near the Tokara Strait (~29.3°N). To the north, the slab is characterised by a steep 70° dip down to 80 km depth, at which point the slab bends sharply (see lower panels of Fig. 1); the southern section of the slab does not bend as sharply, and dips at shallower angles of about 40–50°. This segmentation of the slab near the Tokara Strait requires the presence of a major accommodation structure, such as a tear fault (Nagamune 1987; Kao and Chen 1991). The deepest occurrence of seismicity becomes shallower northwards from ~250 km at 25.5°N (Sibuet et al. 1998) to ~120 km at 33°N (Ishihara and Yoshida 1992).

The morphology and nature of the Philippine Sea Plate is complicated by the presence of many basins, remnant arcs, and ridges. The north-western part of the plate (the area relevant to this study) includes the Amami Plateau, Daito Ridge, and Oki-Daito Ridge. These ridges represent the oldest section of the Philippine Sea Plate; they have been interpreted as parts of a Late Cretaceous to Palaeocene island arc system (e.g. Hilde and Lee 1984). The Amami Plateau has begun to collide with the arc around 28°N (Tokuyama et al. 1985), producing rapid uplift (1–2 mm/year) of the limestone island of Kikai-jima; radiometric dating of the limestone has indicated that the uplift began during the late Quaternary (Konishi et al. 1978). The Kyushu-Palau Ridge (~40–50 Ma) is a splintered remnant of the Izu-Bonin Arc resulting from opening of the Shikoku back-arc basin.

The Late Cretaceous–Tertiary Shimanto Belt (or terrane) extends along the Pacific side of the outer zone of south-western Japan (see review by Isozaki 1996). It is the youngest major orogen of Japan and results from accretion of trench fill sediments and minor ocean-derived lithologies, most of the rocks being metamorphosed to zeolite (and locally greenschist) facies. All the volcanic centres of southern Kyushu and northern Ryukyu are erupted through the Shimanto Belt (Fig. 2), whereas the volcanoes of the central Ryukyus lie on an older (Early Cretaceous) accretionary terrane. Ocean bottom seismographic (OBS) profiling (Iwasaki et al. 1990) has revealed that the crustal thickness is ~25 km beneath the northern Ryukyu arc and ~30 km beneath southern Kyushu.

Marginal basin

The Okinawa Trough is a young back-arc basin formed behind the Ryukyu arc-trench system, by extension within the Eurasia continental lithosphere (e.g. Letouzey and Kimura 1986; Sibuet et al. 1987, 1995). The width of the trough increases from 10 km in the south to more than 200 km in the north. Several en-echelon extensional grabens have been identified within the active central rift along the axis of the trough (Fig. 1), which extends northward into the Shimabara Graben in NW Kyushu where Unzen volcano is currently active. Geophysical measurements (seismic profiling, gravity, magnetism, sea beam and heat flow) acquired in the Okinawa Trough, coupled with dredged samples have revealed that the crust is of continental origin and that its thickness increases from ~18 km in the south to ~30 km in the north (e.g. Iwasaki et al. 1990; Hirata et al. 1991; Sibuet et al. 1995). The Okinawa Trough is still in the early rifting stage of back-arc basin development prior to true spreading. Following Sibuet et al. (1995), three phases of extension can be identified on the basis of refraction/reflection experiments, seismic correlations with drilling stratigraphy and ages of dredged/drilled samples: (1) middle to late Miocene, (2) early Pleistocene, and (3) late Pleistocene to Recent. The second rifting phase is thought to be the most important for producing the present configuration of the Okinawa Trough. Although back-arc magmatism concurrent with the first stage extension is yet to be identified, the second stage opening of the middle Okinawa Trough resulted in abundant volcanic activity that started ~1.5 Ma in the axial zone of the back-arc basin (Shinjo et al. 1999).

Samples studied

We have undertaken a detailed east–west (across-arc) and north–south (along-arc) sampling of Quaternary volcanic rocks in the southern Kyushu and north-central Ryukyu arc to identify spatial variations in the mantle sources of mafic magma supplying this arc. In order to minimise potential compositional variations caused by shallow-level processes such as fractional crystallisation and crustal contamination (see below), we present only basalt to basaltic andesite compositions ($SiO_2 < 56$ wt%; MgO typically 4–6 wt%) from each volcano. For this reason, andesites from Sakurajima, one of the most active volcanoes in southern Kyushu (Fig. 2), are not included in this paper.

Samples are grouped by geographic area; i.e. volcanic front and back-arc in south Kyushu, northern and southern segments in north Ryukyus, and central Ryukyus (Table 1).

Analytical methods

All chemical analyses were undertaken on fresh chips of rock. Samples were initially washed and rinsed with distilled water, and an aliquot of oven-dried chips was then reduced to powder by grinding in an agate ball mill.

Major element compositions were measured on fused glass beads, following standard XRF methods at the Tohoku University. Trace element concentrations were determined by inductively coupled plasma mass spectrometry (Yokogawa Analytical Systems HP4500) at the University of the Ryukyus, with a ^{115}In internal standard, and calibrated with JB-1 (Geological Survey of Japan) standard solutions. Samples were digested in a $HF–HClO_4$ mixture before being dried down, converted to nitrates, and diluted by a factor of 2,000 before being introduced into the instrument.

Sr, Nd and Pb isotope analyses were undertaken at the University of Melbourne. Rock chips (typically ~0.5–1.0 mm) for isotopic analysis were selected by careful hand-picking. These were washed in ultra-pure water and then leached with hot (~80 °C) acid (4 N HCl for Sr and Nd; 6 N HCl for Pb) for 1 h. The chips were then rinsed prior to dissolution in HF and HNO_3. Sr, Nd and Pb were separated by standard ion exchange methods and loaded on single Ta (Sr), Re–Ta double (Nd), and single Re (Pb) filament assemblies. Isotope measurements were made on a Finnigan MAT262 multiple collector mass spectrometer and normalised to $^{86}Sr/^{88}Sr = 0.1194$ and $^{146}Nd/^{144}Nd = 0.7219$. Pb isotope ratios were corrected for mass fractionation by the use of a $^{207}Pb–^{204}Pb$ double-spike (Woodhead et al. 1995). Sr and Nd isotope ratios of some samples, which were prepared separately, were also analysed at the University of the Ryukyus, on a Finnigan MAT262. During the period of this study, measurements for the NIST Standard SRM-987 gave $^{87}Sr/^{86}Sr = 0.710297$ and 0.710307 (Melbourne) and 0.710237 ($n = 5$; Ryukyus), and for the La Jolla Nd Standard, values of $^{143}Nd/^{144}Nd = 0.511833$ and 0.511854 (Melbourne) and 0.511850 ($n = 9$; Ryukyus). Ratios measured for NIST Pb Standard SRM-981 were $^{206}Pb/^{204}Pb = 16.934$, $^{207}Pb/^{204}Pb = 15.491$, and $^{208}Pb/^{204}Pb = 36.698$.

Results

Major and trace element compositions

Analytical data for representative samples are provided in Table 1. On a K_2O vs SiO_2 diagram (Fig. 3), the majority of rocks fall in the medium-K calc-alkaline basalt to basaltic andesite field. Samples from the back-arc region tend to have higher K_2O contents than the volcanic front lavas, with one high-K basalt (NK01). Along the volcanic front, the K_2O contents of the rocks tend to increase northward. Total alkali ($Na_2O + K_2O$) contents are largely between 2 and 5 wt% in the basalts and basaltic andesites. On an alkali vs silica diagram (not shown), the majority of rocks fall in the sub-alkaline field of MacDonald and Katsura (1964), except for the back-arc basalt NK01 from south Kyushu, which plots in the alkaline field. Most rocks have relatively low MgO (typically 4–6 wt%), Cr (< 120 ppm) and Ni (< 42 ppm) contents, and many contain phenocrysts of olivine, clinopyroxene and plagioclase. In most volcanic centres, basalts are rare.

The N-MORB-normalised incompatible element patterns for representative samples are shown in Fig. 4a, which, for comparison, also includes basalts from NW Kyushu (Nakamura et al. 1990), a typical ocean-island basalt (OIB; Sun and McDonough 1989), and an average Nankai Trough sediment (Plank and Langmuir 1998). Because a major source of sediment for this area is south-west Japan, we consider the Nankai Trough sediment as representative of those sediments subducting beneath both south Kyushu and the northern Ryukyu arc.

Most samples are characterised by high abundances of the large ion lithophile elements (LILE), Th and U, positive Pb anomalies, negative Nb–Ta anomalies, and low absolute abundances of high field strength elements (HFSE). These features are typical of subduction-related magmas. Likewise, typical Nankai Trough sediment is strongly enriched in the LILE, the light rare earth elements (LREE) and Pb, and depleted in Nb, P and Ti: characteristics that are shared with most of the volcanic rocks. In contrast, basalt NK01 from the back-arc of south Kyushu is distinct with an enrichment in HFSE similar to the OIB-like basalts from NW Kyushu. Subtle enrichment of LILE is also characteristic of the NW Kyushu basalts (Nakamura et al. 1985, 1990). Chemical differences are also apparent in the REE data (Fig. 4b), which show a distinctive LREE-enriched pattern for OIB-like basalts [NK01 and HOKU8; $(La/Yb)_N = 4.5$–8.9] from the south Kyushu back-arc region relative to the other 'arc-type' rocks that have flat to slightly LREE-enriched patterns [$1.3 < (La/Yb)_N < 3.7$]. Slight negative or positive Eu-anomalies are found in some samples. Note that sample AK3 from Akusekijima in the southern segment of north Ryukyu, has significantly depleted heavy REE content.

Pb, Sr and Nd isotopic compositions

The isotope data are presented in Table 2, and have also been plotted on various covariation diagrams in Figs. 5 through 10. These diagrams also include several reference fields and the hypothetical OIB end members

Table 1 Major and trace element data for Quaternary basalts and basaltic andesites from the northern Ryukyu arc. Major elements were recalculated on H_2O-free basis; original sum range from 98 to 101 wt%

	South Kyushu; volcanic front								Back-arc		North Ryukyu; North segment			South segment						Central Ryukyu			
Sample wt%	KR01	KR03	HOK U41	HOK U43	HOK U33	HOK U34	KIM1	OND	NK01	HOK U8	IWO3	KC4	MK R2	KU C5	NA K13	SU W13	SU W14	AK3	AK34	YOK1	YOK4	TR2	TR12
SiO_2	50.84	50.45	51.50	51.41	48.08	48.84	52.54	51.84	51.54	54.14	51.12	53.95	55.45	55.11	53.40	53.13	53.75	54.65	54.99	53.57	52.45	50.87	55.35
TiO_2	0.73	0.76	0.80	0.80	0.99	1.03	1.11	0.94	1.17	0.89	0.80	0.66	0.78	0.65	0.65	0.68	0.74	0.76	0.64	0.68	0.69	0.74	0.82
Al_2O_3	21.73	18.14	18.52	18.78	18.01	18.42	17.94	17.81	16.65	17.71	18.91	18.66	19.16	18.85	19.46	17.58	17.79	17.96	17.99	19.21	20.49	19.58	17.27
Fe_2O_3	9.33	10.96	9.96	10.02	12.41	12.19	10.94	10.75	9.29	8.24	10.54	9.30	8.14	9.10	9.44	9.73	10.03	9.32	8.86	9.94	9.46	10.97	11.04
MnO	0.16	0.18	0.17	0.17	0.19	0.18	0.20	0.15	0.17	0.13	0.18	0.15	0.15	0.16	0.17	0.16	0.17	0.16	0.15	0.17	0.17	0.18	0.19
MgO	4.16	5.15	5.39	5.14	6.19	5.42	4.32	5.78	6.55	5.53	5.11	4.59	3.82	3.52	4.04	5.04	4.53	4.73	4.72	3.63	4.53	4.81	3.45
CaO	8.98	10.72	10.85	10.69	11.60	10.92	8.91	9.02	9.03	9.22	10.15	8.66	7.71	7.83	8.30	10.35	9.44	8.66	8.88	8.51	8.64	10.60	9.02
Na_2O	2.88	2.82	2.18	2.36	2.01	2.41	3.05	2.57	3.56	2.91	2.60	2.71	3.14	3.48	3.38	2.35	2.78	2.72	2.71	3.25	2.75	1.95	2.39
K_2O	1.08	0.71	0.55	0.51	0.42	0.49	0.79	1.00	1.74	1.03	0.47	1.22	1.53	1.23	1.07	0.90	0.73	0.95	1.00	0.93	0.73	0.22	0.40
P_2O_5	0.11	0.12	0.09	0.12	0.10	0.09	0.21	0.14	0.31	0.20	0.11	0.08	0.13	0.08	0.10	0.07	0.05	0.08	0.07	0.11	0.09	0.06	0.06
ppm																							
Sc	29.3	34.6	37.0	39.2	45.1	41.0	28.8	36.5	24.8	28.8	37.0	31.8	25.6	28.5	27.5	36.4	34.3	66.7	61.4	31.3	34.5	40.6	43.4
V	283	311	327	376	390	394	266	312	197	238	341	259	221	261	256	274	316	515	559	238	250	308	332
Cr	25	42	116	42	12	12	10	81	213	120	45	35	42	4	13	43	8	42	48	15	24	31	12
Co	25	31	31	31	43	36	23	35	34	27	33	32	20	24	24	29	28	55	54	27	30	34	30
Ni	13	18	26	12	18	7	5	21	103	42	20	21	10	6	9	15	11	16	41	12	16	10	4
Rb	33.0	18.7	13.8	12.8	9.2	8.4	17.9	20.4	51.8	20.1	11.5	33.1	50.2	30.6	21.8	21.2	14.6	29.4	34.2	28.4	23.1	5.7	12.4
Sr	313	343	316	304	336	355	267	592	386	362	285	245	238	215	228	235	251	272	270	174	160	133	138
Y	15.9	16.3	16.9	21.4	19.4	18.6	33.1	21.6	22.0	24.1	15.8	17.9	23.1	18.5	18.7	18.7	16.9	22.3	20.9	23.7	21.3	17.4	20.4
Zr	70	52	59	66	45	59	107	74	137	152	45	81	111	64	58	57	51	82	70	84	70	32	54
Nb	2.9	2.3	3.8	2.7	3.6	3.3	5.0	2.9	47.6	13.2	1.5	2.6	4.4	2.2	1.2	1.6	1.4	3.1	2.3	3.0	2.5	1.3	1.7
Cs	2.15	1.07	0.72	0.78	0.47	0.35	0.85	0.53	0.52	0.71	0.50	1.27	1.84	1.61	1.23	1.14	0.63	1.06	0.82	1.44	1.46	0.22	0.74
Ba	196	153	126	105	100	113	134	174	660	276	93	178	229	157	132	111	103	114	106	127	105	38	66
Hf	1.98	1.53	1.55	1.76	1.26	1.53	2.92	2.03	3.06	3.47	1.21	2.22	2.81	1.81	1.80	1.50	1.36	1.01	0.87	2.27	1.91	0.92	1.51
Ta	0.24	0.18	0.23	0.15	0.22	0.21	0.31	0.21	2.88	0.82	0.11	0.23	0.35	0.19	0.10	0.14	0.12	0.11	0.11	0.23	0.19	0.09	0.14
Pb	5.96	6.00	3.97	3.83	2.17	2.36	5.77	5.23	4.24	5.69	4.55	6.95	6.74	7.79	7.30	5.77	5.36	3.62	4.07	9.93	6.86	1.86	2.58
Th	2.95	1.73	1.16	0.89	0.80	0.90	1.89	2.43	6.37	2.97	1.04	3.11	4.92	2.16	1.45	1.64	1.08	0.99	0.89	2.47	1.99	0.59	1.37
U	0.73	0.42	0.28	0.23	0.18	0.20	0.43	0.59	1.13	0.61	0.27	0.84	1.01	0.65	0.56	0.46	0.33	0.28	0.29	0.74	0.60	0.15	0.35
La	8.54	7.46	6.17	6.44	5.20	5.14	11.10	11.15	31.39	16.25	5.18	7.57	13.36	6.73	4.93	5.22	3.76	5.47	5.08	8.56	6.99	3.44	4.82
Ce	19.10	17.13	13.56	15.78	12.27	12.01	28.67	25.45	54.00	33.79	12.36	17.14	27.06	15.81	12.50	12.40	8.69	12.61	11.26	20.17	16.61	8.04	11.70
Pr	2.37	2.18	1.83	2.23	1.80	1.71	3.97	3.37	5.64	4.09	1.62	2.13	3.52	2.02	1.75	1.64	1.18	1.54	1.41	2.58	2.16	1.17	1.56
Nd	10.38	10.05	8.37	10.47	8.67	8.08	18.21	14.81	21.89	16.67	7.76	9.39	15.01	9.15	8.58	7.73	5.77	6.75	6.17	11.77	9.97	5.84	7.50
Sm	2.63	2.65	2.27	2.88	2.58	2.37	4.81	3.60	4.33	3.77	2.19	2.41	3.53	2.46	2.52	2.14	1.75	1.76	1.62	3.12	2.72	1.85	2.29
Eu	0.84	0.90	0.90	1.00	0.99	0.97	1.46	1.11	1.39	1.21	0.79	0.74	0.98	0.76	0.79	0.72	0.78	0.55	0.50	0.87	0.80	0.68	0.78
Gd	2.84	2.97	2.52	3.19	2.96	2.71	5.38	3.61	4.38	3.89	2.54	2.85	3.82	2.89	3.01	2.63	2.22	2.04	1.89	3.63	3.25	2.32	2.83
Tb	0.48	0.49	0.43	0.54	0.51	0.48	0.89	0.58	0.69	0.63	0.45	0.49	0.64	0.50	0.54	0.47	0.41	0.33	0.31	0.63	0.58	0.44	0.54
Dy	2.97	3.01	2.74	3.44	3.15	2.98	5.58	3.55	3.90	3.82	2.80	3.08	3.92	3.12	3.38	2.86	2.60	1.97	1.81	3.96	3.64	2.88	3.49
Ho	0.64	0.65	0.59	0.73	0.68	0.65	1.18	0.75	0.83	0.81	0.61	0.66	0.84	0.69	0.73	0.61	0.56	0.42	0.39	0.88	0.80	0.64	0.77
Er	1.87	1.93	1.73	2.15	1.96	1.89	3.47	2.16	2.36	2.41	1.76	2.04	2.42	2.02	2.18	1.86	1.76	1.22	1.13	2.60	2.38	1.97	2.34
Tm	0.30	0.30	0.27	0.33	0.29	0.29	0.54	0.34	0.37	0.37	0.27	0.31	0.37	0.32	0.34	0.30	0.28	0.19	0.17	0.40	0.37	0.29	0.35
Yb	1.94	1.92	1.70	2.07	1.83	1.83	3.41	2.10	2.37	2.43	1.74	2.09	2.39	2.09	2.20	1.88	1.84	1.16	1.07	2.61	2.39	1.83	2.24
Lu	0.30	0.29	0.26	0.32	0.27	0.28	0.53	0.32	0.35	0.37	0.27	0.32	0.38	0.33	0.34	0.27	0.27	0.18	0.17	0.41	0.37	0.29	0.35

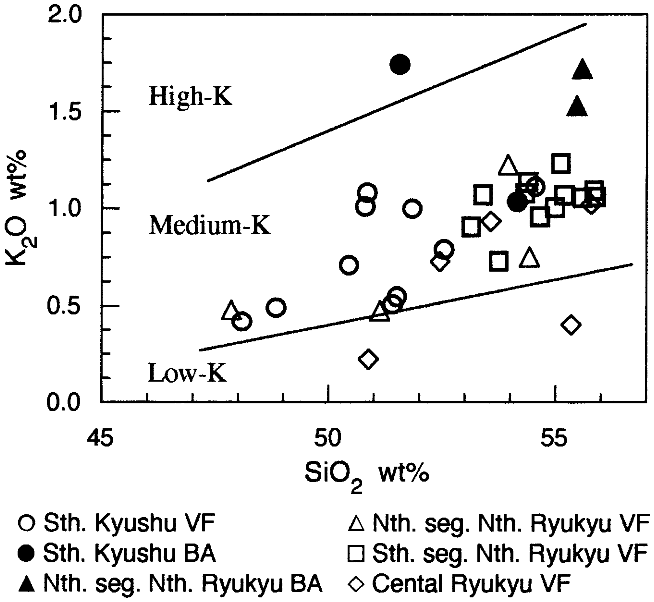

Fig. 3 K_2O vs SiO_2 diagram for the mafic rocks from the northern Ryukyu arc. High-, medium- and low-K discriminants are from Le Maitre et al. (1989). The samples are grouped into six geographic suites. *Open* and *solid symbols* represent rocks from volcanic front (*VF*) and back-arc (*BA*), respectively

enriched mantle type I (EMI) and EMII of Hart (1988) to allow comparison with rocks in known tectonic settings and locales.

Figure 5 illustrates the Pb-isotopic compositions of the samples. The $^{206}Pb/^{204}Pb$ ratios of the lavas range from 18.22 to 18.49, $^{207}Pb/^{204}Pb$ from 15.53 to 15.61, and $^{208}Pb/^{204}Pb$ from 38.26 to 38.67, lying distinctly above the Northern Hemisphere Reference Line (NHRL) of Hart (1984). The new data clearly define two distinct trends that converge at high values of $^{206}Pb/^{204}Pb$ (Fig. 5c, d). One of these projects back into the field for Pacific MORB (defined by the NHRL) and includes samples from the northern Ryukyu volcanic front, whereas the other trend projects into the field for Indian Ocean MORB and includes samples from the south Kyushu volcanic front and back-arc. Basalts from the central Ryukyus (i.e. Yokoate-jima and Iwotori-shima) have the highest $^{208}Pb/^{204}Pb$ and $^{207}Pb/^{204}Pb$. The data for samples from the northern segment of the north Ryukyus fall in transitional fields between the two trends described above: sample MKR2 from the back-arc island of Kuro-shima plots in the south Kyushu data field. These two distinct trends in Pb isotope space are similar to those of Lau Basin lavas first described by Hergt and Hawkesworth (1994).

The $^{87}Sr/^{86}Sr$ of lavas ranges from 0.7038 to 0.7052; $^{143}Nd/^{144}Nd$ from 0.5126 to 0.5129. In the $^{87}Sr/^{86}Sr$ vs $^{143}Nd/^{144}Nd$ plot (Fig. 6), data for volcanic front lavas from the north and central Ryukyu arc show a systematic shift to high $^{87}Sr/^{86}Sr$ relative to south Kyushu lavas. There is an overall negative trend, particularly well developed in the south Kyushu lavas. The data for samples from the northern segment of north Ryukyu fall in transitional fields between the two trends described above. Note that the Sr–Nd isotope composition of basalt NK01 overlaps with the field of intraplate-type basalts from NW Kyushu (Nakamura et al. 1990).

Discussion

Crustal assimilation and differentiation processes

Prior to assessing potential magma sources, we need to evaluate the effects of post-melting processes such as fractional crystallisation and crustal contamination. Although we limit our discussion to basalts and basaltic andesites with < 56 wt% SiO_2, there appear to be no truly primitive rocks in this region; all mafic rocks reported here have typically 4–6 wt% MgO and low Ni and Cr contents.

In Fig. 7a, our $^{87}Sr/^{86}Sr$ data are compared with all other available data spanning the basalt to rhyolite compositional spectrum: this figure indicates that the basalts and basaltic andesites reported here generally possess the lowest Sr isotope ratios.

Crustal contamination generally results in the simultaneous increase of SiO_2, incompatible elements, and decrease of most compatible elements (e.g. MgO). An example of this can be found in the variation from basalts through andesites to rhyolites from the Aira Caldera (Fig. 7b–d; data from Arakawa et al. 1998). Here substantial contamination leads to higher $^{87}Sr/^{86}Sr$ ratios, which correlate positively with SiO_2 and negatively with MgO content. At the compositional range (SiO_2 < 55 wt%; MgO > 3 wt%) of rocks reported in this paper, there is no apparent correlation between Sr–Nd isotopes, SiO_2, and MgO (Fig. 7b, c). Moreover, we find that there is no significant difference in incompatible element ratios (e.g. Ba/Zr; Fig. 7e) between less fractionated basalts and more fractionated samples within volcanoes in the northern Ryukyu arc. Finally, the Aira Caldera samples show a positive correlation between $^{87}Sr/^{86}Sr$ and Th/La (Fig. 7d), whereas these ratios in the mafic rocks from this study are rather scattered and do not follow the contamination trend. These observations suggest that the variations in chemical and isotopic compositions recorded in our samples do not result from crustal contamination, but reflect mantle source characteristics and processes. Because the basalts and basaltic andesites used are unavoidably somewhat evolved, we mainly use incompatible-element and isotopic ratios (which do not change appreciably during closed-system magmatic differentiation processes) in the following discussion of source region characteristics.

Source characteristics

The data presented in this paper clearly confirm the well-established concept that arc magmas have a complex multi-source origin, including the mantle wedge and

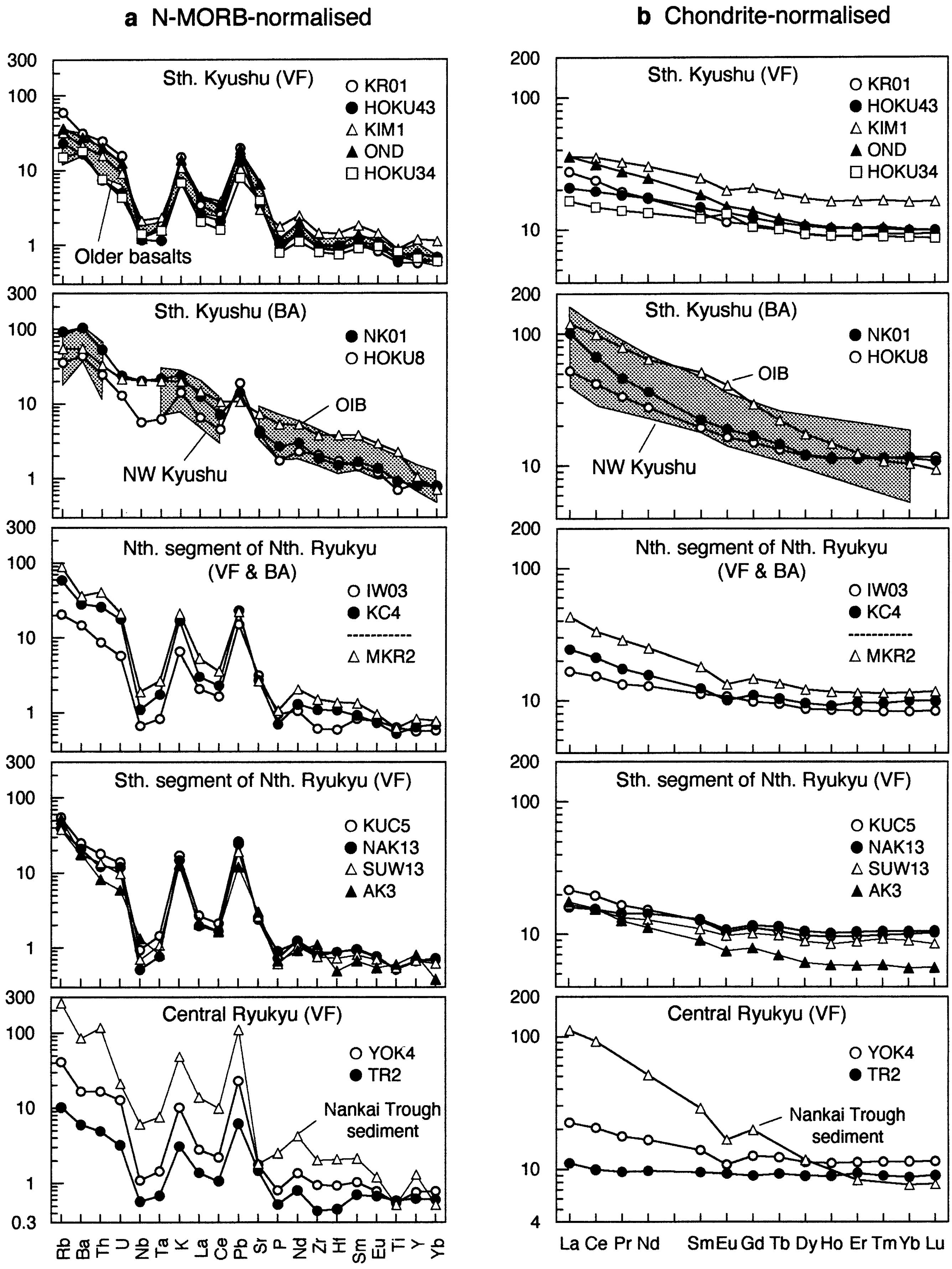
a N-MORB-normalised
b Chondrite-normalised
Sth. Kyushu (VF)
KR01
HOKU43
KIM1
OND
HOKU34
Older basalts
Sth. Kyushu (BA)
NK01
HOKU8
OIB
NW Kyushu
Nth. segment of Nth. Ryukyu
(VF & BA)
IW03
KC4
MKR2
Sth. segment of Nth. Ryukyu (VF)
KUC5
NAK13
SUW13
AK3
Central Ryukyu (VF)
YOK4
TR2
Nankai Trough sediment
Rb Ba Th U Nb Ta K La Ce Pb Sr P Nd Zr Hf Sm Eu Ti Y Yb
La Ce Pr Nd Sm Eu Gd Tb Dy Ho Er Tm Yb Lu
300
100
10
1
0.3
200
10
4

◄

Fig. 4 **a** N-MORB (Sun and McDonough 1989) normalised-incompatible element diagrams for representative mafic rocks from the northern Ryukyu arc. Most lavas are characterised by enrichments of LILE (Ba, U, K, Sr) over HFSE (Th, Nb, Ta, Zr, Ti), and LREE-enrichment. The exception is basalt NK01 (and to some extent HOKU8) from back-arc of south Kyushu, which are similar to intraplate-type basalts from NW Kyushu (Nakamura et al. 1990). **b** Chondrite-normalised REE patterns (Boynton 1984) for representative mafic rocks from the northern Ryukyu arc. The composition of the average sediment (Nankai Trough) being subducted beneath the northern Ryukyus (Plank and Langmuir 1998), typical ocean-island basalt (OIB; Sun and McDonough 1989), and the older basalts from the Hisatsu (Nagao et al. 1999) and Hokusatsu (R. Shinjo unpublished data) volcanic provinces are also shown for comparison

various subduction components. Most importantly, our Pb isotope data define two distinctly separate but convergent trends (Fig. 5), reflecting mixing of these components. These are, in our preferred model, Pacific and Indian MORB-like mantle and subduction components (fluids, sediment and altered oceanic crust), although the extrapolated position of mixing components A–C in Fig. 5 may not represent the exact isotopic compositions of these end members.

Component A in Fig. 5 has high $^{207}Pb/^{204}Pb$ and $^{208}Pb/^{204}Pb$ consistent with an upper crustal influence. This feature is most readily explained by recent recycling of sediment derived from the subducting Philippine Sea plate. The Ryukyu sediments reported by Sun (1980) represent the best analogue for such material. Although distinction from derivation by melting of sub-continental lithosphere (as discussed below) is difficult, it seems more likely that this radiogenic Pb signature was introduced directly into the source by subduction of sediments.

In a plot of Ba/Nb vs Sr, Nd and Pb isotopes (Fig. 8), however, the arc rocks do not fall on a simple mixing line between sediments and mantle wedge (the latter inferred from typical MORB). This suggests that, in addition to the sediment component noted above, excess Ba (and other LILE) in the volcanic front lavas are derived from an additional, unradiogenic source. Experimental data have shown that Ba, Pb, Sr, U and K are highly fluid mobile whereas Th and Nb behave

Table 2 Sr, Nd, and Pb isotopic data for basalts and basaltic andesites from the northern Ryukyu Arc. Data in italics are obtained at University of the Ryukyus, others at the University of Melbourne. Uncertainties for Sr and Nd isotopic ratios correspond to the last two digits. The CHUR parameter used for εNd *calculation* is 0.512638

Sample	Lat. (°N)	Long. (°E)	Location	$^{87}Sr/^{86}Sr$	$^{143}Nd/^{144}Nd$	εNd	$^{206}Pb/^{204}Pb$	$^{207}Pb/^{204}Pb$	$^{208}Pb/^{204}Pb$
South Kyushu; volcanic front									
KR01	31°53′	130°54′	Kirishima	0.704759 ± 15	0.512564 ± 07	−1.4	18.272	15.560	38.422
KR03	31°53′	130°54′	Kirishima	0.704807 ± 14	0.512572 ± 07	−1.3	18.280	15.572	38.455
HOKU41	31°39.2″	130°36.4′	Yoshinodai	*0.704610 ± 17*	*0.512710 ± 06*	1.4			
HOKU43	31°41.3′	130°36.5′	Yoshinodai	0.704579 ± 18	0.512685 ± 10	0.9	18.296	15.563	38.421
				0.704679 ± 14	*0.512703 ± 08*	1.3			
HOKU33	31°45.8′	130°33.5′	Sumiyoshi-ike	*0.704154 ± 15*	*0.512803 ± 09*	3.2			
HOKU34	31°46.2′	130°34.7′	Sumiyoshi-ike	0.703925 ± 13	0.512832 ± 07	3.8	18.215	15.537	38.257
				0.703897 ± 13	*0.512866 ± 08*	4.4			
KIM1	31°11′	130°32′	Kaimon-dake	0.705140 ± 13	0.512561 ± 15	−1.5	18.374	15.588	38.555
				0.705174 ± 16					
OND	31°14.5′	130°31′	Ohno-dake	0.703902 ± 16	0.512698 ± 08	1.2	18.275	15.556	38.360
				0.703974 ± 16					
South Kyushu; back-arc									
NK01	31°46.4′	130°28.5′	Nakayama	0.703834 ± 12	0.512837 ± 07	3.9	18.270	15.533	38.393
HOKU8	31°47.6′	130°24.5′	Maruyama	0.704264 ± 16	0.512721 ± 08	1.6	18.301	15.560	38.429
				0.704254 ± 18	*0.512768 ± 09*	2.5			
North segment of north Ryukyu; volcanic front									
IWO3	30°47′	130°17.5′	Iwo-jima (Kikai Caldera)	0.704822 ± 17	0.512711 ± 08	1.4	18.405	15.563	38.420
KC4	30°27′	130°13′	Kuchinoerabu-jima	0.704338 ± 12	0.512763 ± 10	2.4	18.415	15.558	38.375
North segment of north Ryukyu; back-arc									
MKR2	30°49′	129°55′	Kuro-shima	0.704398 ± 15	0.512714 ± 08	1.5	18.392	15.589	38.550
South segment of north Ryukyu; volcanic front									
KUC5	29°58′	129°56′	Kuchino-shima	0.704725 ± 15	0.512760 ± 06	2.4	18.462	15.559	38.406
NAK13	29°51′	129°52′	Nakano-shima	0.704262 ± 17	0.512914 ± 08	5.4	18.455	15.545	38.321
SUW13	29°38′	129°43′	Suwanose-jima	0.704923 ± 14	0.512714 ± 13	1.5	18.474	15.572	38.456
SUW14	29°38′	129°43′	Suwanose-jima	0.704745 ± 13	0.512744 ± 10	2.1	18.482	15.559	38.397
AK3	29°27′	129°36′	Akuseki-jima	0.704942 ± 20	0.512687 ± 12	1.0	18.475	15.581	38.513
Central Ryukyu; volcanic front									
YOK4	28°47.5′	129°00′	Yokoate-jima	0.704942 ± 15	0.512690 ± 08	1.0	18.494	15.609	38.674
TR2	27°52′	128°14′	Iwotori-shima	0.705208 ± 12	0.512747 ± 10	2.1	18.459	15.613	38.673
				0.705173 ± 23	*0.512735 ± 11*	1.9			

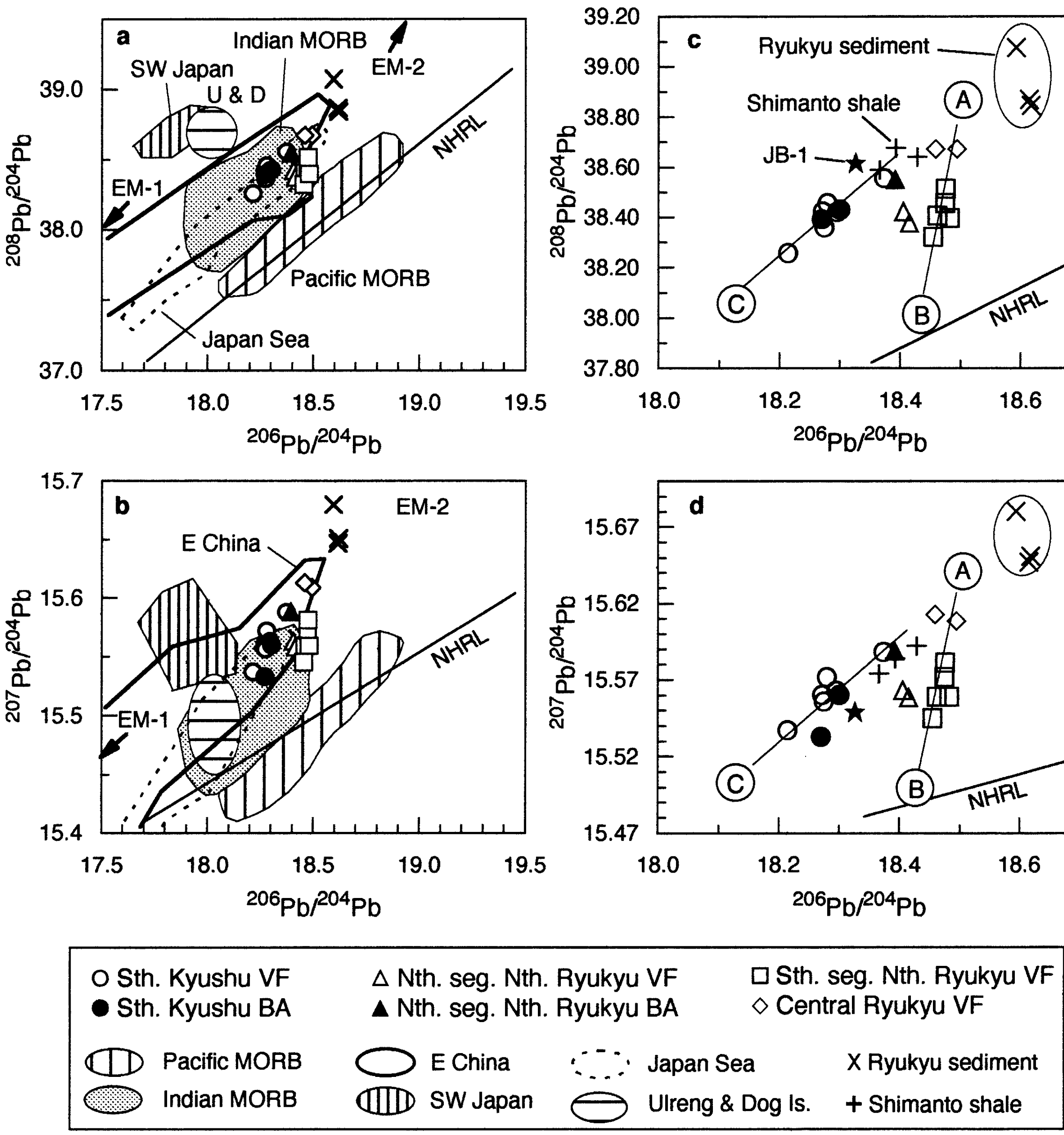

Fig. 5 Conventional Pb isotope diagram. **a**, **b** Comparisons of Ryukyu arc data with regional data. **c**, **d** Detail for the Ryukyu arc. MORB data are compiled from Mahoney et al. (1992) and references therein. The Northern Hemisphere Reference Line (NHRL; Hart 1984) and compositions of mantle components (enriched mantle: EM-1 and EM-2; Hart 1988) are shown for reference. Also shown are Ryukyu sediments (Sun 1980), Japan Sea basalts (Tatsumoto and Nakamura 1991; Cousens and Allan 1992; Cousens et al. 1994), Shimanto shale (Ishikawa and Nakamura 1994), SW Japan (Kurasawa 1968), E China (Peng et al. 1986), post-opening Japan Sea islands (*U&D* Ulreng and Dog islands; Tatsumoto and Nakamura 1991), and JB-1 (typical intraplate-type basalt of NW Kyushu; Shimoda and Nohda 1995). Note that the data form two distinct linear trends. *Letters A–C* in **c** and **d** show the isotopic components discussed in the text

as immobile HFSE (e.g. Keppler 1996). Thus the high Ba/Nb component in Fig. 8 is inferred to be aqueous fluid derived from the subducting slab, as suggested by recent studies in a number of other arcs (e.g. Turner et al. 1998). From Fig. 8 we can see that the $^{87}Sr/^{86}Sr$ and $^{207}Pb/^{204}Pb$ of this fluid component are significantly less radiogenic than those of subducting sediments. However these are attributes that might be expected of fluids expelled from the dehydration of altered oceanic crust (AOC), which is our preferred interpretation.

Component B in Fig. 5 appears to be similar to Pacific MORB-type asthenospheric mantle (as defined by the NHRL). We note, however, that a number of authors have argued against an asthenospheric influence for this signature. For instance, Kersting et al. (1996) favour a lithospheric mantle source for arc magmatism in NE Japan. This possibility, however, can be ruled out for the following reasons.

First, the volcanic centres lie on a young (Cretaceous to Tertiary) accreted terrane, the Shimanto Belt. Given this situation, metasomatism of the base of the lithosphere by subduction-related processes may have

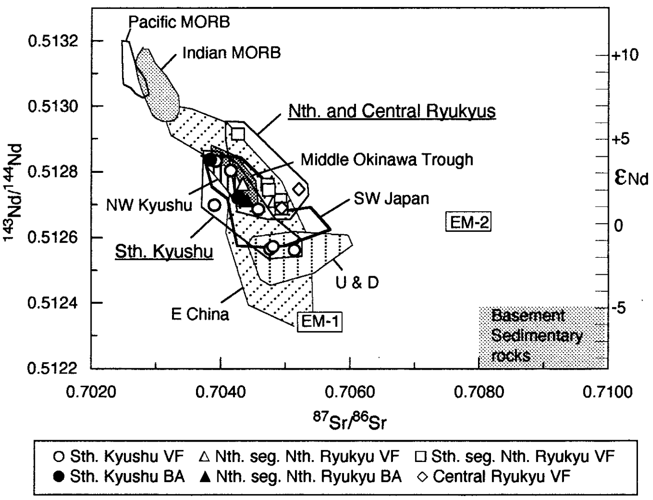

Fig. 6 $^{87}Sr/^{86}Sr$ vs $^{143}Nd/^{144}Nd$ diagram for Ryukyu arc sample suite and comparisons with regional data. Data sources are included in those given in the caption to Fig. 5; in addition, the Quaternary basalts from the middle Okinawa Trough (Shinjo et al. 1999), basalts from NW Kyushu (Nakamura et al. 1990), and Cretaceous to Palaeocene granites and sediments from SW Japan (Terakado et al. 1988; Arakawa et al. 1998) are shown

occurred and, if this is the case, the subarc subduction-modified lithosphere should have an 'upper crustal' isotopic imprint (e.g. high $^{87}Sr/^{86}Sr$ and $^{208}Pb/^{206}Pb$), in contrast to the MORB-like signature seen. Tatsumoto and Nakamura (1991), Tu et al. (1992) and Chung et al. (1995) have also proposed the presence of an isotopically enriched subcontinental lithosphere in the Japan Sea, NW Taiwan, and South China Sea region. Studies by Tatsumoto et al. (1992) demonstrate that such signatures may be preserved for hundreds of millions of years.

In addition, because both lithospheric extension and magma production are inferred to be significant in south Kyushu (discussed below), isotopic signals from the lithospheric mantle would be expected to be more common here than in the northern Ryukyu arc. However, our data for the south Kyushu lavas indicates no contribution from such component.

Finally, we argue that the composition of the subducting sediments and overriding lithosphere should be uniform over this restricted, along-strike transect from south Kyushu to the north Ryukyus. This leaves the asthenospheric mantle as the only remaining petrogenetic variable. As a result of all these considerations, we propose that end-member B observed in the Pb isotope data is most likely Pacific MORB asthenosphere.

Component C in Fig. 5 resembles Indian Ocean MORB-type mantle and the so-called 'east Asian low velocity composition' (i.e. $^{206}Pb/^{204}Pb$ ~17.6–18.8, $^{87}Sr/^{86}Sr$~0.7035–0.7040, and $^{143}Nd/^{144}Nd$~0.5129–0.5130) proposed by Hoang and Flower (1998) and Flower et al. (1998) for the shallow low-velocity mantle sampled by east Asian volcanism. These authors proposed that this signature reflects EM1-enriched asthenosphere with small additions of fluid and sediment melt from the subducting slab. The similarity of DUPAL-like east Asian and western Pacific asthenosphere to Indian Ocean MORB has been noted by several workers (e.g. Hickey-Vargas et al. 1995; Castillo 1996). Divergent opinions for the origin of their Pb signatures currently prevail, including the influx of Indian Ocean mantle (e.g. Mukasa et al. 1987; Hickey-Vargas et al. 1995; Castillo 1996), endogenous mantle plumes (Tatsumoto and Nakamura 1991), and delaminated cratonic substrate (Hoang et al. 1996; Flower et al. 1998; Smith 1998). It is believed that the extreme EMI- or EMII-rich compositions (outside the 'east Asian low velocity composition' field) observed in rocks from eastern China, islands in the Japan Sea, and Hainan island reflect complex interaction of asthenosphere and EMI- and/or EMII-rich lithosphere (Basu et al. 1991; Tatsumoto and Nakamura 1991; Tatsumoto et al. 1992).

Although a detailed discussion concerning the origin of 'Indian-like' Pb isotope signature for east Asian basalts is beyond the scope of this paper, we would suggest that the asthenosphere, yielding 'Indian-like' or 'DUPAL-like' Pb isotopes, postulated for many east Asian margin magmas is not necessarily derived from exactly the same source as Indian Ocean MORB, and may have a distinct origin. For example, most magmas from the region share the compositional features of OIB, and are not as depleted as Indian Ocean MORB. Second, the majority of basalts from east China and the Japan Sea, which have 'Indian MORB-like' Pb isotopes, do not plot in the Indian MORB field of the Sr–Nd isotopic diagram. In addition, on the basis of integration of Sr and Nd isotopic data for various types of igneous rocks from SW Japan, Terakado et al. (1997) suggested maximum epsilon-Nd values of about +3 for this area. All of these observation are inconsistent with derivation from a mantle source exactly identical to that of Indian Ocean MORB. In addition, because of the large variation in Pb isotope ratios observed for Pacific and Indian MORB (Fig. 5), any estimation of the size of the slab-derived component (sediment + AOC-derived fluid) involved in Kyushu–Ryukyu volcanism is limited by an inability to assess accurately the Pb isotope ratio of the mantle wedge beneath the arc.

As an alternative model for explaining the two distinct trends in the Pb isotopic data (Fig. 5), one could interpret these trends as mixing arrays between a fixed mantle source and two distinct subduction zone components. In such a model, slabs subducting beneath south Kyushu and the north-central Ryukyus should be of Indian and Pacific-type, respectively.

Lavas from the Eocene–Miocene Philippine Sea Plate basins, including the Daito, West Philippine, Shikoku and Parece Vela basins, do have elevated $^{208}Pb/^{204}Pb$ and somewhat elevated $^{207}Pb/^{204}Pb$ compared with NHRL, characteristics of Indian Ocean MORB-type mantle (Hickey-Vargas 1991, 1998). However, note that lavas from the Kyushu-Palau Ridge (Arc), Daito Ridge, and Amami Plateau are clearly isotopically distinct from

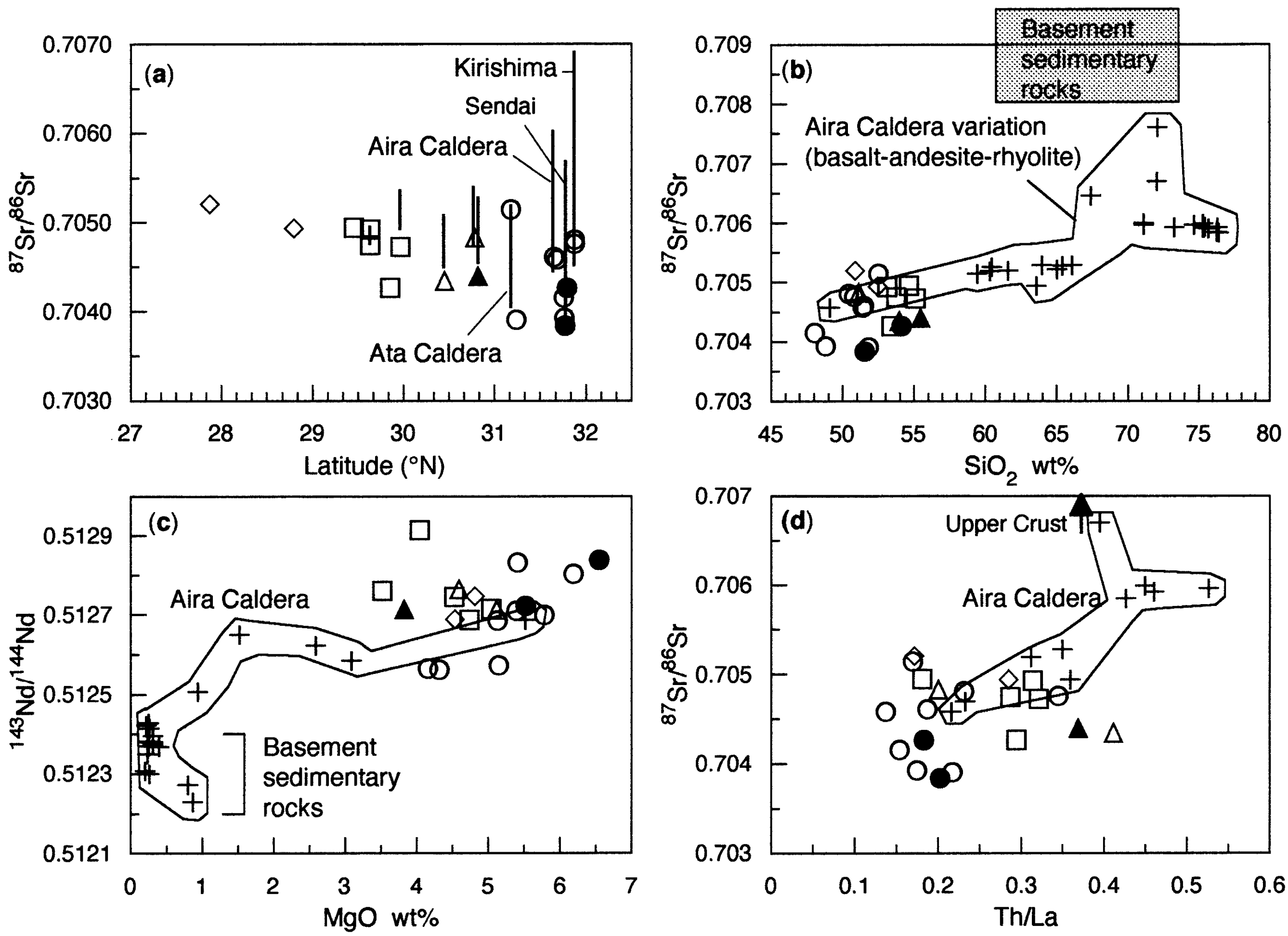

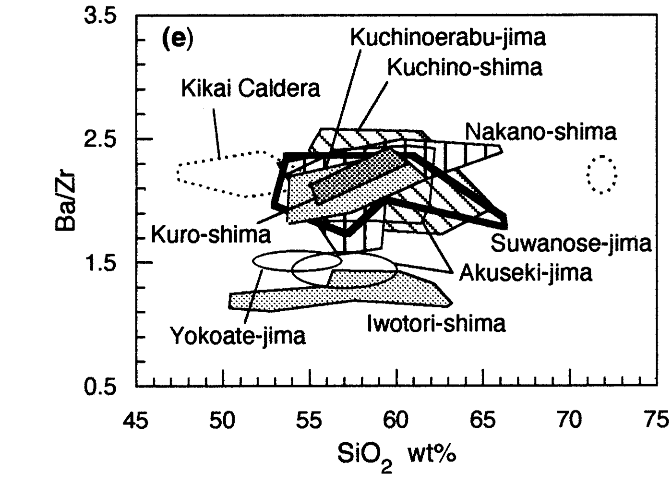

Fig. 7 **a** $^{87}Sr/^{86}Sr$ variation with latitude. *Bars* indicate the range of compiled data from Notsu et al. (1990, reference therein) and Arakawa et al. (1998; except for minor dark pumices having $^{87}Sr/^{86}Sr$ of 0.7065–0.7076). **b** $^{87}Sr/^{86}Sr$ vs SiO_2 diagram. Compositional range from basalt to rhyolite from the Aira caldera is based on data of Tsukui and Aramaki (1990) and Arakawa et al. (1998). Field for basement sedimentary rocks from Arakawa et al. (1998). **c** $^{143}Nd/^{144}Nd$ vs MgO diagram. **d** $^{87}Sr/^{86}Sr$ vs Th/La diagram. Average upper continental crust (Th/La = 0.36) from Taylor and McLennan (1985). **e** Ba/Zr vs SiO_2 diagram for northern Ryukyu lavas. Data sources: Nakada (1986), Tiba (1989), and unpublished data compilations of R. Shinjo (1999)

basin lavas; most volcanic rocks from these ridges plot close to the NHRL and have Pb-isotope ratios similar to modern Pacific plate MORBs (see Fig. 8 of Hickey-Vargas 1998). Unfortunately there are no available isotopic data for rocks from the area between the Kyushu-Palau Ridge and Amami Plateau, the area corresponding to the slab subducting beneath both south Kyushu and north Ryukyu. However, because Pacific-type Pb signatures dominate in samples from the Kyushu-Palau, Amami, and Daito Ridges, it is natural to infer that the oceanic crust of the slab subducted beneath both south Kyushu and north-central Ryukyus also has Pacific-type Pb.

To investigate this possibility further, we plot Ba/Nb vs $^{206}Pb/^{204}Pb$ for our samples (Fig. 8d). In this figure, we use typical $^{206}Pb/^{204}Pb$ values for Pacific and Indian MORB mantle (and AOC) as estimated from Fig. 5. Fluids released from the dehydration of the AOC should

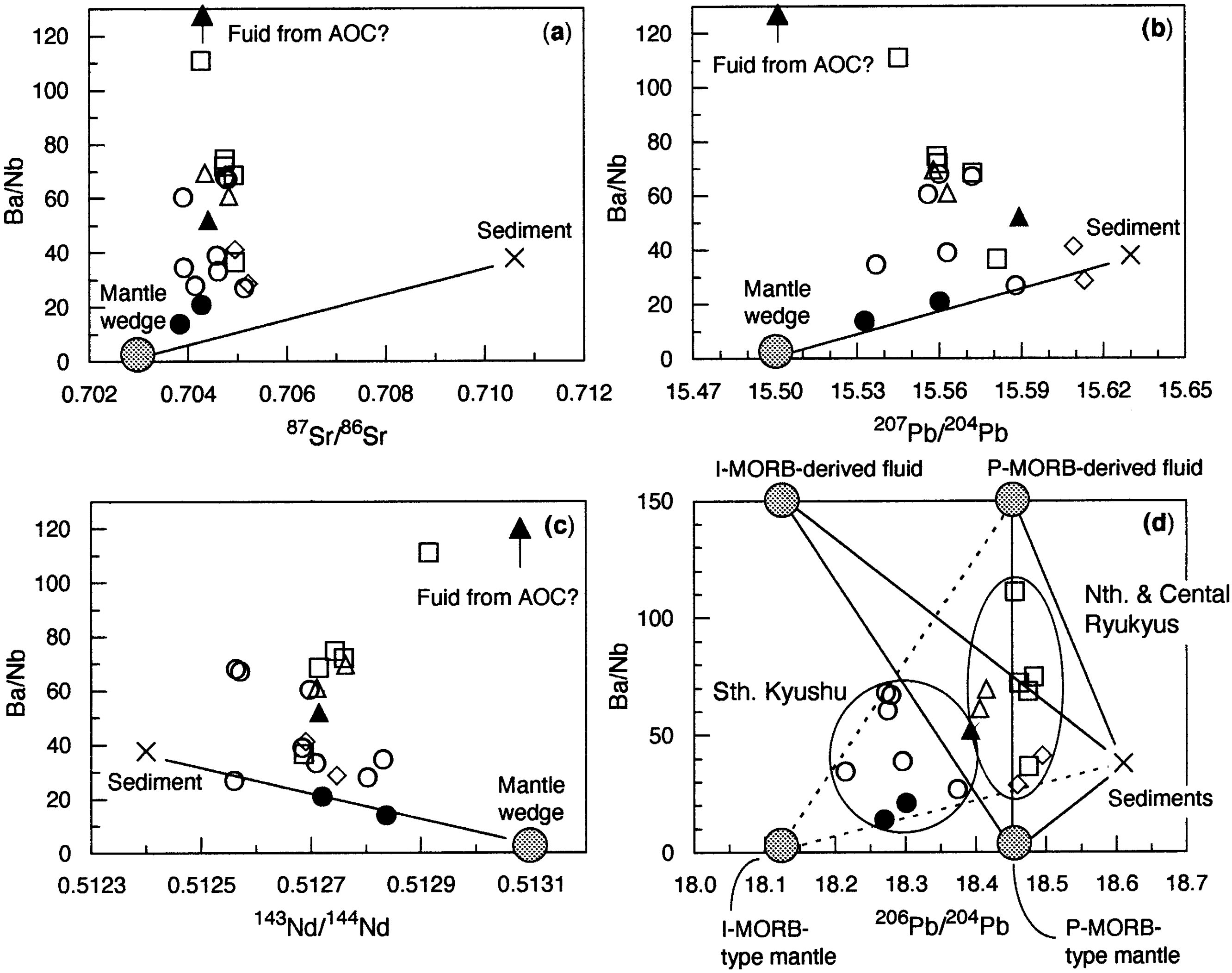

Fig. 8 **a** Ba/Nb vs $^{87}Sr/^{86}Sr$, **b** $^{207}Pb/^{204}Pb$, **c** $^{143}Nd/^{144}Nd$, and **d** $^{206}Pb/^{204}Pb$ diagrams, showing requirement of a fluid component (from altered oceanic crust: AOC) as well as the mantle wedge and subducted sediments. Symbols are the same as those in Fig. 5. The sediment is assumed to have $^{207}Pb/^{204}Pb = 15.63$, $^{206}Pb/^{204}Pb = 18.61$ (an average of Ryukyu sediments reported in Sun 1980), $^{87}Sr/^{86}Sr = 0.7106$ (an average of Cretaceous to Palaeocene granites and sediments from SW Japan; Terakado et al. 1988), $^{143}Nd/^{144}Nd = 0.5124$, and Ba/Nb = 37.7 (Nankai Trough sediment from Plank and Langmuire 1998). I-MORB, Indian Ocean MORB; P-MORB, Pacific MORB

be enriched in Ba (thus high Ba/Nb) but have $^{206}Pb/^{204}Pb$ similar to unaltered MORB. This is because the Nd and Pb isotope ratios of MORB are insensitive to low temperature seawater interaction, as a result of low concentrations of Nd and Pb in seawater (e.g. Cousens et al. 1994). We tentatively estimate Ba/Nb for an AOC-derived fluid as high as 150, which is similar to Ba/Nb = 133 for average oceanic arc basalt (McCulloch and Gamble 1991). Ryukyu lavas can be reproduced by three component mixing involving Pacific MORB-type mantle, Pacific MORB (AOC)-derived fluid, and sediment, because the data fall within this ternary system. On the other hand, Kyushu data seem to be difficult to explain with three components including Pacific MORB-type mantle, Indian MORB (AOC)-derived fluid, and sediment. Kyushu data require an additional low $^{206}Pb/^{204}Pb$ and low Ba/Nb component, i.e. an Indian MORB-type mantle. A three component model including Indian MORB-type mantle, Pacific MORB (AOC)-derived fluid, and sediment, can easily account for the Kyushu data. We therefore prefer the former model in which two distinct mantle reservoirs are involved in magmagenesis within the region.

The debates concerning the origin of Indian MORB-like Pb signatures in east Asian basalts aside, the existence of two groups of lavas that show distinct Pb–Sr–Nd isotopic systematics (Figs. 5 and 6) is by far the most significant geochemical feature of the northern Ryukyu arc. The geographical distribution of these two groups suggests that the magmas in south Kyushu and north Ryukyu tapped distinct mantle domains. Because samples from the back-arc island of Kuro-shima in the north Ryukyus have Pb–Sr–Nd isotopes that fall in the south Kyushu fields (Figs. 5 and 6), we may estimate the present day boundary between Indian Ocean MORB-type and Pacific MORB-type mantle domains to be present between Kuro-shima and the volcanic front volcanoes in the northern segment. Further south, the lack of Pb isotope data for lavas from the back-arc side (e.g. middle Okinawa Trough area; Fig. 1) makes delineation of the southward extension of this boundary difficult. The middle Okinawa Trough basalts have Sr and Nd isotopic ratios similar to south Kyushu basalts (Fig. 6). Because Shinjo et al. (1999) proposed E-MORB type (or OIB type) asthenospheric mantle involvement in these magma sources, Indian Ocean-like asthenosphere may extend further south in the Okinawa Trough region.

Geochemical variation along the volcanic front in the north-central Ryukyus

Although mafic magmas of the northern Ryukyu volcanic front define a isotopic mixing trend between Pacific MORB-type mantle wedge and subduction components (sediment + fluids), a significant geochemical variation exists along-strike within the volcanic front (Figs. 4–6). In Fig. 9 we examine trace element and isotope variations with latitude. Magmas from the central Ryukyus are distinct in having generally lower Ba/La, Ba/Th, and $^{143}Nd/^{144}Nd$, and higher $^{207}Pb/^{204}Pb$, $^{87}Sr/^{86}Sr$, and Ce/Pb than magmas from the north Ryukyus.

We suggest that these compositional changes reflect variable sediment and/or fluid fluxes from the subducting slab. Although regional variation in isotopic compositions of sediments may be responsible for the along-arc chemical variation, this possibility is difficult to evaluate because of the lack of relevant sediment data.

If we assume the mantle wedge is broadly uniform in composition along of the northern Ryukyu volcanic front, then the variation in subduction-sensitive ratios in Fig. 9 should reflect variation in the subduction component (e.g. Plank and Langmuir 1993).

Pb is well known to be extremely mobile during dehydration processes in the subducting slab (Keppler 1996; Kogiso et al. 1997), whereas Nb (and Ta) are highly immobile. The ratio of their concentrations thus monitors the slab signature with great sensitivity. In a $^{207}Pb/^{204}Pb$ vs Ta/Pb diagram (Fig. 10a), the north-central Ryukyu front lavas can be interpreted in terms of mixing between sediment and a fluid from altered oceanic crust (AOC). In this model, the variation in Pb isotopes (and possibly also in $^{87}Sr/^{86}Sr$ and $^{143}Nd/^{144}Nd$) observed for these lavas is interpreted in terms of different sediment/AOC ratios. In contrast to the north-central Ryukyu lavas, the volcanic front lavas of south Kyushu define a poor negative correlation between $^{207}Pb/^{204}Pb$ and Ta/Pb. This may indicate that the Sr, Nd and Pb isotope compositions of the fluids involved in these magmas are relatively homogeneous.

We can estimate the relative contributions of sediment components to the source region (Fig. 10b) using the following simplifying assumptions: (1) depleted mantle has Pb and Ce concentrations 10 times lower than average MORB (Pb = 0.3 ppm, Ce = 7.5 ppm; Sun and McDonough, 1989), (2) mantle has isotope ratios similar to those of typical Pacific MORB (i.e. $^{207}Pb/^{204}Pb = 15.5$; Stolper and Newman 1994), (3) MORB/fluid partition coefficients are ~0.05 for Pb and ~11 for Ce (Brenan et al. 1995), and (4) 2 wt% of fluid is expelled from AOC (Brenan et al. 1995). The results of this simple model suggest that the AOC-derived fluid contributes between 50 and 95 wt% to the slab-derived component and that the sediment contribution is dominant for the central Ryukyu lavas (40–50 wt%) and lower in the north Ryukyu lavas (5–20 wt%). We must not forget that the subducting slab is not uniform in character along its length, as previously described. Large, buoyant ridges on the subducting plate such as the Amami Plateau are a characteristic feature in the north Ryukyus, while, in the southern part, the oceanic crust of the West Philippine Basin subducts relatively easily. The buoyant nature of the Amami Plateau contributes to its preservation relative to normal oceanic crust; sediment offscraping forms the recent accretionary prism in the northern part, but such a sediment fill is absent at the trench in the south (Iwasaki et al. 1990). This contrast probably limits the amount of sediment subducted in the northern region.

Therefore we conclude that along-arc variations in the compositions of the northern Ryukyu lavas were inherited from heterogeneities in the slab-derived component; the regional variation in geochemical compositions can be explained by a greater sediment contribution in the sources of southern segment magmas relative to their northern counterparts.

Chemical heterogeneity in south Kyushu magmas

Mixtures of Indian Ocean-type mantle and Ryukyu sediment can account for the isotopic variation of lavas erupted in south Kyushu (Fig. 5). Lower incompatible trace element concentrations and lower La/Yb in the arc front lavas compared with back-arc lavas is consistent with the arc front lavas originating by larger degrees of partial melting. Concurrent decrease in the involvement of subduction components in passing westward suggests that this may in part reflect higher volatile contents beneath the volcanic front leading to increased mantle melting.

However, even if a slab-derived component is dominant in the source of arc front magmas compared with that of back-arc magmas, there are significant differences in the nature of the wedge itself. The arc front lavas, like many of their counterparts worldwide, are characterised by a depletion in HFSE and HREE, not only relative to the LIL elements but also in absolute terms, reflected in sub-MORB abundances of these elements (Fig. 4). These distinctions between the volcanic front and back-arc basalts exceed those that can be

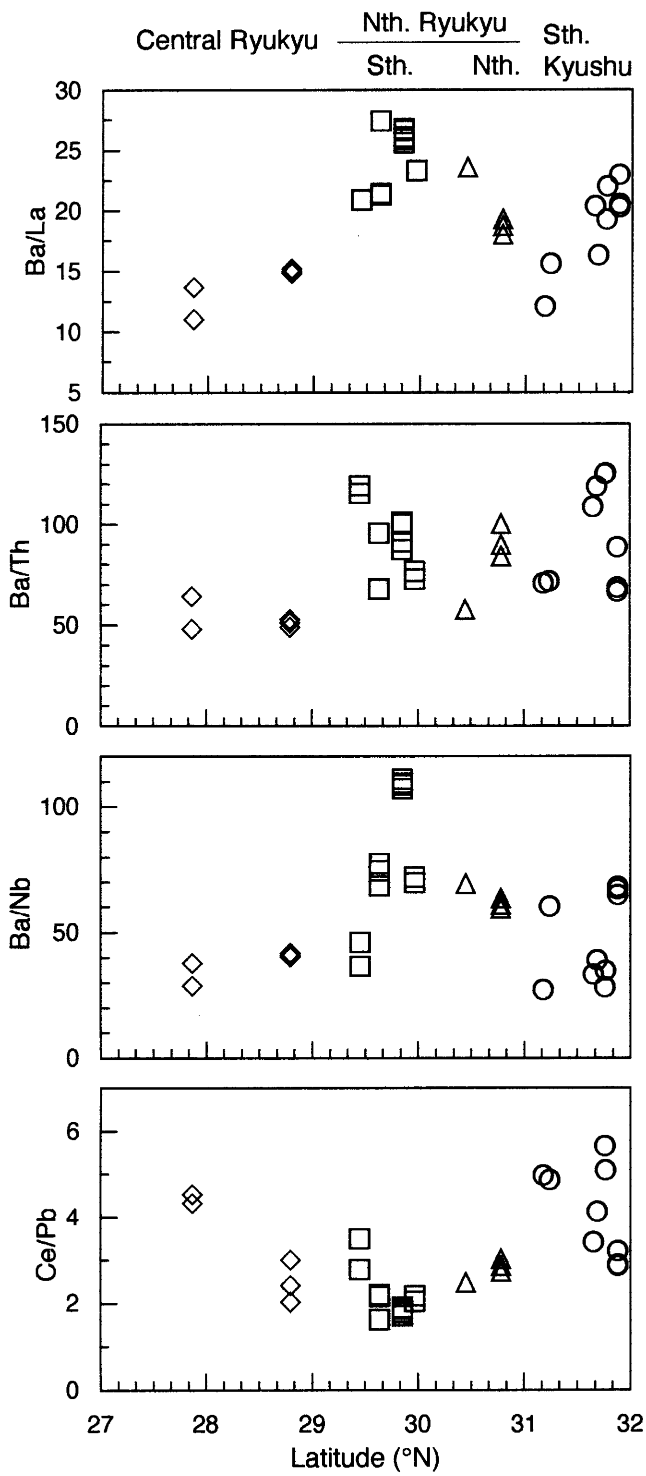

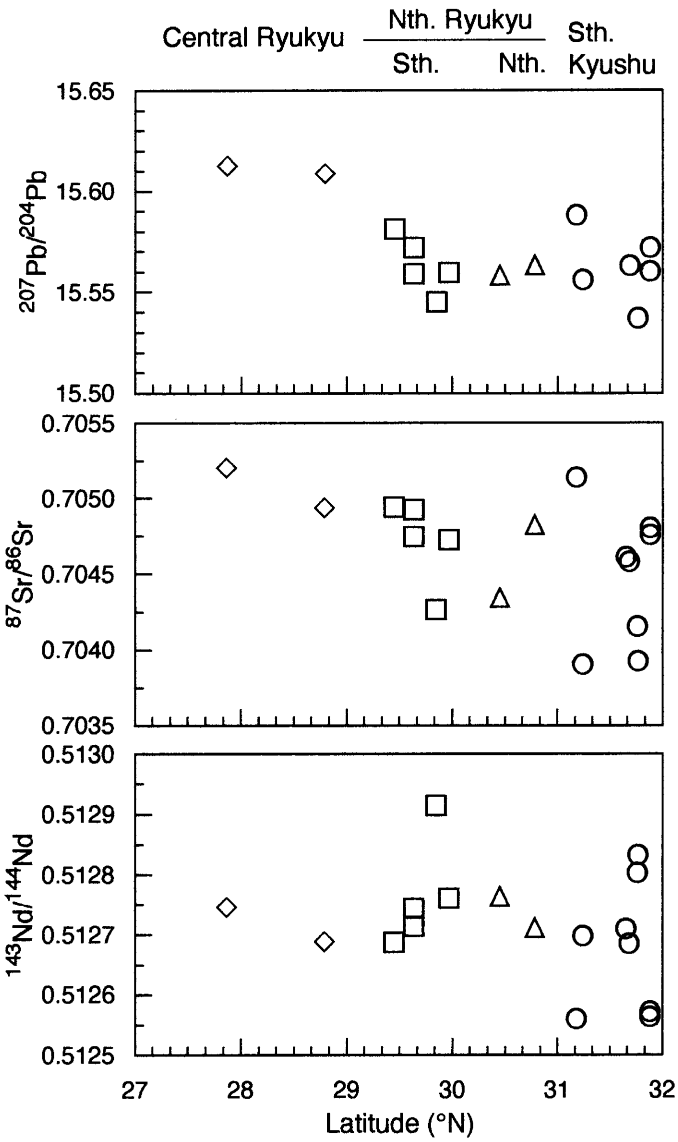

Fig. 9 Latitudinal variations of trace element ratios (Ba/La, Ba/Th, Ba/Nb, and Ce/Pb) and Pb–Sr–Nd isotopic ratios in lavas along the volcanic front of the northern Ryukyu arc. Basalts from the volcanic front of south Kyushu are also shown for comparison

caused by variations in present day mantle melting. Experimental data and interpretations of trace element abundances for arc magmas suggest that there is little or no enrichment of HFSE related to subduction processes, such that the HFSE are derived largely from the mantle wedge (Tatsumi et al. 1986; Pearce and Peate 1995). Examination of the relative abundances of these fluid-immobile, yet incompatible trace-elements in order of increasing residual-mantle compatibility (Nb > Zr > Hf; see Fig. 4) indicates that ratios of less compatible to more compatible elements (e.g. Nb/Zr, Zr/Hf) are lower in arc-front magmas. Low Nb/Zr and Zr/Hf values in arc-front lavas are indicative of magma derivation from a more depleted mantle source (i.e. less fertile) than that sampled by back-arc magmas. Their geochemical compositions, therefore, indicate substantial depletion of the mantle source prior to re-enrichment in LILE by the subduction process. It is speculated

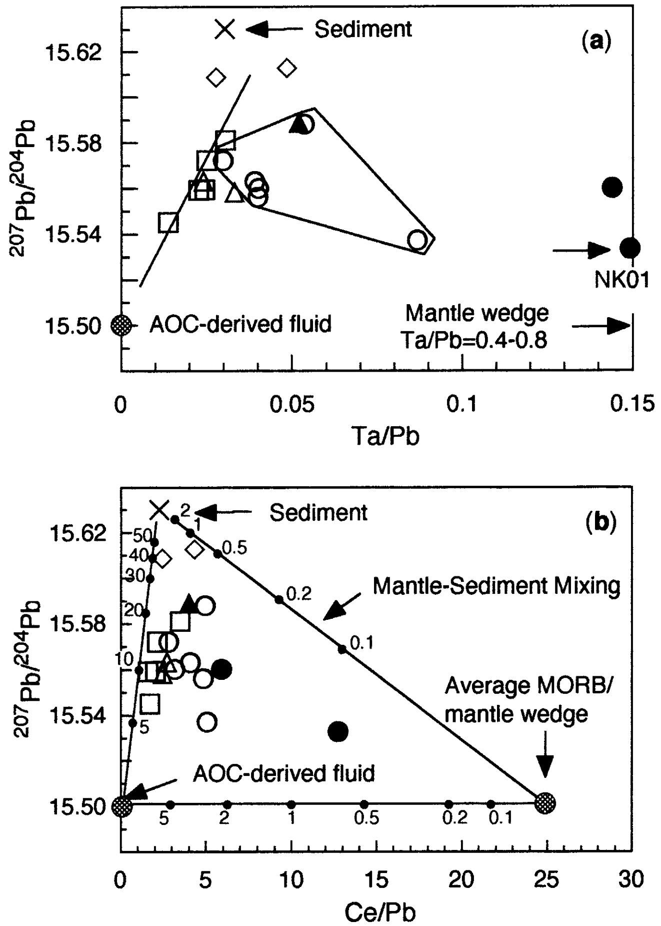

Fig. 10 **a** $^{207}Pb/^{204}Pb$ vs Ta/Pb and **b** Ce/Pb diagrams for isotopic mixing models of mantle wedge, sediment, and altered oceanic crust (AOC) derived fluid. Average MORB (Sun and McDonough 1989; assumed to be equivalent in Ce/Pb and Pb-isotope composition as a MORB-source-type mantle wedge), average sediment (Plank and Langmuir 1998; Sun 1980), and AOC-derived fluid (Ce/Pb calculated using the data in Brenan et al. 1995, 2 wt% fluid evolved from a source with a garnet/clinopyroxene mass ratio of 60/40) are used for calculation. *Numbers on dot marks* correspond to the weight percentage of one end-member in each binary mixture

that this might result from melt extraction associated with volcanic activity in the back-arc, as suggested for the Mariana Trough (Stolper and Newman 1994) and Kamchatka arc (Hochstaedter et al. 1996).

As shown in Fig. 9, the magmas erupted at the volcanic front in south Kyushu have a wide range of incompatible-element and isotope ratios, which are also poorly correlated with distance from the trench (or depth to the slab). Because it is highly unlikely that the slab-derived component is heterogeneous within this very restricted region, this chemical heterogeneity may reflect variable depletion of the mantle wedge making it more susceptible to contamination (e.g. Wallace and Carmichael 1999). In addition, complex tectonomagmatic interactions (see below) involving asthenospheric injection and steepening of the subduction angle might also contribute to the chemical heterogeneity of the mantle wedge.

Finally we note that basalts erupted towards the back-arc of south Kyushu display little or no characteristic ‘subduction’ fingerprint such as HFSE depletion relative to LILE. Indeed in terms of trace element abundances they appear similar to many ocean-island basalts, OIB (see Fig. 4). The appearance of OIB-like magmas within the back-arc of south Kyushu has parallels in the Cascade arc (Borg et al. 1997) and Mexican volcanic belt (Wallace and Carmichael 1999). Note also that the south Kyushu back-arc area is the place where voluminous volcanism occurred from ~8 to ~1 Ma (Fig. 2). The most MgO-rich (~6 wt%) basalts erupted during this period, from the Hisatsu and Hokusatu volcanic fields (Nagao et al. 1999; R. Shinjo unpublished data) have depleted signatures in terms of abundances and ratios of HFSE (Fig. 4), implying that they were derived from depleted sources. HFSE depletion of the local mantle source by melt extraction associated with this older phase of volcanism appears to be inconsistent with recent emplacement of these later HFSE-enriched, OIB-like basalts. Except for a subtle enrichment of LILE and Pb, OIB-like basalt (NK01) from the south Kyushu back-arc has trace element and Sr–Nd–Pb isotopic compositions similar to intraplate-type basalts of NW Kyushu (Figs. 4–6). Thus the source of the back-arc magmas may be more closely linked to the asthenosphere tapped by NW Kyushu basalts that have been erupted since ~12 Ma (Fig. 11a).

A geodynamic interpretation: asthenospheric flow recorded in magmatic activity

The chemistry of lavas erupted in south Kyushu and the northern Ryukyus provides unique insights into mantle dynamics beneath the region, because an interplay between two major mantle domains is apparently recorded by the resulting volcanic activity. There is a strong link between the occurrence of Indian vs Pacific MORB signatures and the nature of the subducting slab in that the Indian signature is only seen in the northern region where the subducted slab bends sharply; to the south of this area Pacific mantle is dominant.

We propose that Indian-type asthenosphere injected eastwards into the mantle wedge of south Kyushu, and that this injection either caused or was induced by the slab bending presently observed below this region. The eastward shift of volcanism in south Kyushu with time (during ~3 to 1 Ma) probably resulted from a gradual steepening in the dip of the subducted slab (Fig. 11c). This asthenospheric domain was responsible for producing OIB-like basalts within the back-arc (Fig. 11d).

Recent geophysical data provide evidence for the existence of upwelling hot asthenosphere. Seismic tomography (e.g. Davis 1996) defines several low-velocity anomalies beneath the Asian continental margin. One of these underlies the southern Japan Sea and appears to coincide with intraplate volcanism in south-western Japan and off NW Kyushu (Fig. 1; see Plate 1 of Flower

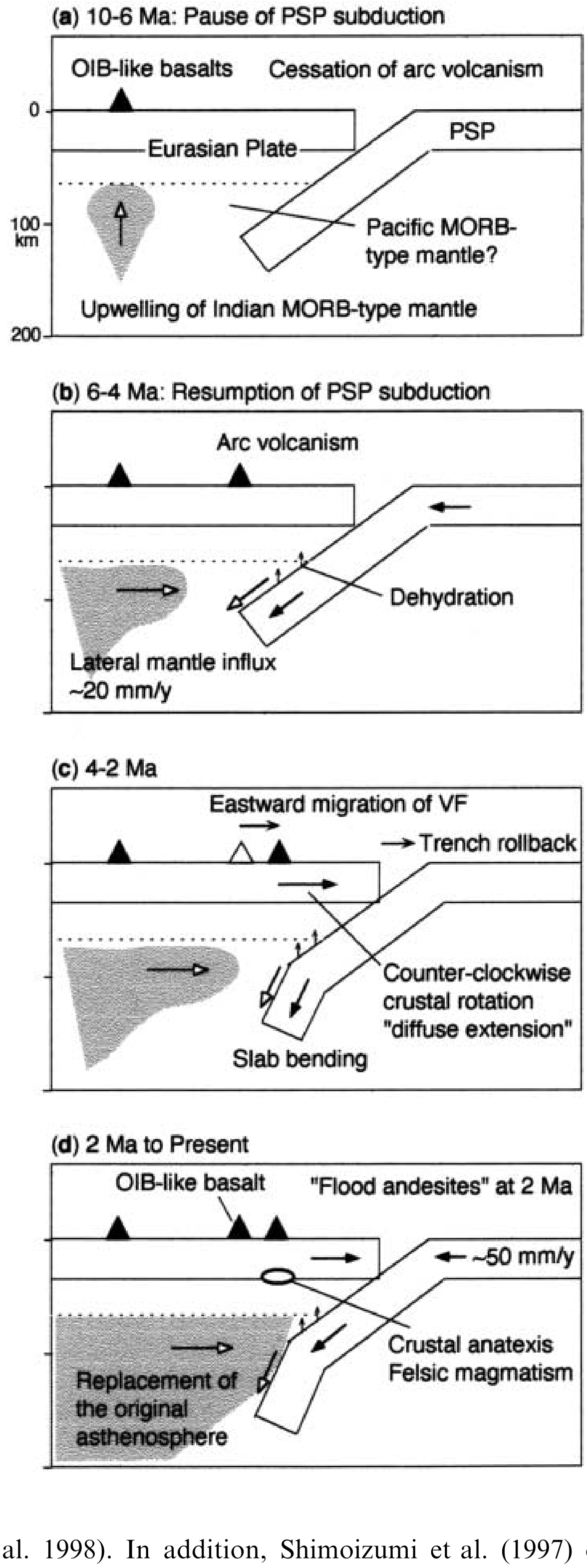

◀

Fig. 11 Illustration of the proposed mantle dynamics in south Kyushu, and the northernmost Ryukyu subduction system. *Open* and *solid arrows* indicate mantle flow and lithospheric movement, respectively. *Solid* and *open triangles* represent active and extinct volcanoes, respectively. **a** At ~10 Ma, the upwelling of asthenospheric mantle, yielding Indian Ocean MORB-type signatures, resulted in intraplate-type basalt magmatism in the NW Kyushu region. Corresponding to a 10–6 Ma halt in subduction of the Philippine Sea Plate (*PSP*), arc volcanism became inactive (Kamata and Kodama 1994). **b** Lateral influx of mantle into the sub-arc wedge. The resumption of PSP subduction led not only to a reactivation arc volcanism, but may also have accelerated eastward asthenospheric flow because of induced flow and viscous drag along the surface of the downgoing plate. Sediment from the slab may be mixed into the wedge assemblage along the interface. **c** During the period 4–2 Ma, the asthenospheric flow caused slab bending, which also resulted in an eastward migration of the volcanic front. In addition, because of the viscous drag force at the base of the overriding lithosphere, south Kyushu experienced counter-clockwise crustal rotation. **d** This configuration promotes not only a rising geotherm in the wedge, but also produces 'flood andesites' at ~2 Ma under an extensional regime. High magma production rates and an elevated geotherm may also cause extensive crustal anatexis producing rhyolite magma and leading to caldera formation. OIB-like basalts are erupted in the back-arc of south Kyushu, beneath which the leading edge of the slab is not present

et al. 1998). In addition, Shimoizumi et al. (1997) defined the presence of a high electric conductivity layer at the depth range of 50–100 km beneath the East China Sea off NW Kyushu, indicative of partial melting. The inferred eastward mantle flow is consistent with focal mechanisms of intermediate-depth earthquakes within the subducted slab that indicate a down-dip extension under the region (e.g. Chiao 1993). On a regional scale, south-eastward asthenospheric flow has been inferred based on the azimuthal anisotropy directions of Montagner and Tanimoto (1991). Additionally, subduction-induced convection (e.g. Davies and Stevenson 1992), by virtue of resumption of the Philippine Sea Plate subduction at 6 Ma (Kamata and Kodama 1994), probably accelerated south-eastward asthenospheric flow.

Based on the time-lag (~10 million years) and distance from the upwelling centre (~200 km; from off NW Kyushu to south Kyushu), we can estimate the rate of south-westward mantle flow to be of the order of ~20 mm/year, which is similar to local plate motions and inferred plume upwelling rates. For example, Tada (1985) has interpreted strain measurement data in terms of an opening of the Unzen Graben at a rate of about 14 mm/year. Thus asthenospheric flow rate may be linked to the rate of motion of the overlying plate.

We suggest that the asthenospheric injection proposed here was the pivotal event in the tectonomagmatic evolution of the Kyushu area, and accounts for a number of geological phenomena: (1) postulated crustal rotation (and diffuse extension) in south Kyushu since 2–3 Ma, (2) appearance of 'voluminous andesite' activity at ~2 Ma in south-western Kyushu, and (3) a distinctive phase of recent volcanism characterised by caldera formation in south Kyushu.

Recent integrations of palaeomagnetic data have revealed that both south Kyushu and the northernmost Ryukyu arc have experienced counter-clockwise rotation with respect to north Kyushu and the Eurasian continent during the past 2–3 million years, accompanied by crustal extension (Kodama and Nakayama 1993; Kamata and Kodama 1994; Kodama et al. 1995). In addition, recent geodetic (GPS) observations reveal that the GPS stations in Kyushu are migrating eastward with velocities of 1–2 cm/year relative to stable Eurasia (Miyazaki et al. 1996). Intra-arc crustal extension has also been suggested by field evidence for normal faulting in south Kyushu (Fabbri et al. 1997). In this respect, we concur with Seno (1999) that the mantle upwelling northwest of Kyushu is driving Kyushu to the east by the viscous drag force exerted on the overriding lithosphere.

The trench-ward asthenospheric influx undoubtedly influences the geothermal structure and stress regime beneath south-western Kyushu. Nagao et al. (1995; 1999) proposed that the 'flood andesites' forming lava plateaus distributed widely throughout the Hisatsu, Hokusatsu, and Nansatsu volcanic zone (Fig. 2) in south Kyushu, were erupted during a relatively short period of $\sim$2 Ma. The trace element patterns and available $^{87}Sr/^{86}Sr$ (0.7049–0.7052: Nagao et al. 1995) data for these andesites are similar to those of the present volcanic front lavas. The occurrence of 'flood andesites' may not only reflect thermal input beneath the region, but also crustal extension.

Quaternary volcanism in south Kyushu is characterised by the eruption of large volumes of silicic magmas (ignimbrites), which eventually produce calderas such as those of Aira and Ata (Fig. 2; e.g. Aramaki 1984). This magmatism differs markedly with the andesite-dominated volcanism in the north-central Ryukyus, and thus a large contrast in magma supply rate and geotherm are inferred. The silicic magmatism is likely to reflect high degrees of crustal contamination or intra-crustal melting (Arakawa et al. 1998), which require extraordinary heat sources. Rising geothermal gradients, associated with increasing magma supply rate, may result in partial anatexis of the crust and lead to volcanism characterised by caldera formation with voluminous crustal melts. The crustal rotation, as described above, possibly caused a change in the stress field from compressional to extensional, which led to long-term storage of silicic magma and thus caldera formation.

Concluding remarks

Quaternary mafic lavas from the northern Ryukyu arc are striking in their heterogeneity. New Pb isotope data indicate that lavas from south Kyushu and the north-central Ryukyus were derived from distinct mantle domains; the former may be derived from mantle of Indian Ocean-type, whereas the later from mantle wedge of Pacific-type. The geochemical variation of mafic magmas along the north-central Ryukyu volcanic front can be explained by greater sediment involvement in the sources of the central Ryukyu magmas. In contrast, back-arc lavas from south Kyushu show a distinct affinity with OIB and resemble NW Kyushu basalts which have been emplaced since $\sim$12 Ma.

It is possible that the OIB-like basalts in the back-arc and the bending of the slab beneath the volcanic front is related to influx of Indian-MORB like asthenosphere into the mantle wedge of south Kyushu. Asthenospheric flow from an upwelling zone beneath NW Kyushu pushed the subducted slab and produced a drag force at the base of overriding lithosphere, which caused the bending of the slab and the extensional crustal rotation. Such a model also explains the complex temporal, spatial, and geochemical patterns of volcanism observed in south Kyushu. Further investigation is required in order to chart the spatial–temporal development of the isotopic character of the south Kyushu volcanic arc.

Acknowledgements We would like to thank H. Fujimaki, T. Ohba and T. Miyamoto (Tohoku University) for assisting with the XRF analyses. R. Shinjo is grateful to Y. Kato (University of the Ryukyus) for encouragement. This research was supported by the Uruma Trust Fund to R.S. and a Overseas Program for Scientific Research (to R.S.) from the Ministry of Education, Science, Sports, and Culture, Japan. Constructive review by P.W. Reiners and comment by a anonymous reviewer are gratefully appreciated.

References

Arakawa Y, Kurosawa M, Takahashi K, Kobayashi Y, Tsukui M, Amakawa H (1998) Sr–Nd isotopic and chemical characteristics of the silicic magma reservoir of the Aira pyroclastic eruption, southern Kyushu, Japan. J Volcanol Geotherm Res 80: 179–194

Aramaki S (1984) Formation of the Aira caldara, southern Kyushu, ~22,000 years ago. J Geophys Res 89: 8485–8501

Basu AR, Junwen W, Wankang H, Guanghong X, Tatsumoto M (1991) Major element, REE, and Pb, Nd and Sr isotopic geochemistry of Cenozoic volcanic rocks of eastern China: implications for their origin from suboceanic-type mantle reservoirs. Earth Planet Sci Lett 105: 149–169

Borg LE, Clynne MA, Bullen TD (1997) The variable role of slab-derived fluids in the generation of a suite of primitive calc-alkaline lavas from the southernmost Cascades, California. Can Mineral 35: 425–452

Boynton WV (1984) Geochemistry of the rare Earth elements: meteorite studies. In: Henderson P (ed) Rare earth element geochemistry, Elsevier, Amsterdam, pp 63–114

Brenan JM, Shaw HF, Ryerson FJ (1995) Experimental evidence for the origin of lead enrichment in convergent-margin magmas. Nature 378: 54–56

Castillo PR (1996) Origin and geodynamic implication of the Dupal isotopic anomaly in volcanic rocks from the Philippine island arcs. Geology 24: 271–274

Chiao L-Y (1993) Strain segmentation and lateral membrane deformation rate of the subducted Ryukyu slab. Island Arc 2: 94–103

Chung S-L, Jahn B-M, Chen S-J, Lee T, Chen C-H (1995) Miocene basalts in northwestern Taiwan: evidence for EM-type mantle sources in the continental lithosphere. Geochim Cosmochim Acta 59: 549–555

Cousens BL, Allan JF (1992) A Pb, Sr, and Nd isotopic study of basaltic rocks from the Sea of Japan, ODP Leg 127/128. In: Tamaki K, Suyehiro K, Allan J et al. (eds) Proc ocean drilling program sci results 127/128, College Station, TX (Ocean Drilling Program), pp 805–817

Cousens BL, Allan JF, Gorton MP (1994) Subduction-modified pelagic sediments as the enriched component in back-arc basalts from the Japan Sea: ocean drilling program sites 797 and 794. Contrib Mineral Petrol 117: 421–434

Daishi M, Hayashi M, Kato Y (1987) Radiometric ages of some Cenozoic volcanic rocks from Ryukyu Islands. J Jpn Assoc Mineral Petrol Econ Geol 82: 370–381

Davies JH, Stevenson DJ (1992) Physical model of source region of subduction zone volcanics. J Geophys Res 97: 2037–2070

Davis PM (1996) Tomography and seismic anisotropy of Asia and present and past tectonics. In: Yin A, Harrison TM (eds) The

tectonic evolution of Asia. Cambridge Univ Press, Cambridge, pp 85–94
Fabbri O, Tokushige H, Hayamizu M (1997) Normal faulting in the Middle Miocene Osumi granodioritic pluton, southern Kyushu, Japan, and its significance. J Geol Soc Jpn 103: 141–151
Flower M, Tamaki K, Hoang N (1998) Mantle extrusion: a model for dispersed volcanism and DUPAL-like asthenosphere in east Asia and the western Pacific. In: Flower MFJ, Chung S-L, Lo C-H, Lee T-Y (eds) Mantle dynamics and plate interactions in East Asia. AGU Geodynamics 27: 67–88
Flower MFJ, Zhang M, Chen C-Y, Tu K, Xie G (1992) Magmatism in the South China Basin, 2. Post-spreading Quaternary basalts from Hainan Island, south China. Chem Geol 97: 65–87
Hart SR (1984) A large-scale isotope anomaly in the southern hemisphere mantle. Nature 309: 753–757
Hart SR (1988) Heterogeneous mantle domains: signatures, genesis and mixing chronologies. Earth Planet Sci Lett 90: 273–296
Hergt JM, Hawkesworth CJ (1994) Pb-, Sr-, and Nd-isotopic evolution of the Lau Basin: implications for mantle dynamics during backarc opening. In: Hawkins J, Parson L, Allan J, et al. (eds) Proc ocean drilling program sci results 135, College Station, TX (Ocean Drilling Program), pp 505–517
Hickey-Vargas R, Hergt JM, Spadea P (1995) The Indian Ocean-type isotopic signature in western Pacific marginal basins: Origin and significance. In: Taylor B, Natland J (eds) Active margins and marginal basins of the western Pacific. AGU Monogr 88: 175–197
Hirata N, Kinoshita H, Katao H, Baba H, Kaiho Y, Koresawa S, Ono Y, Hayashi K (1991) Report on DELP 1988 cruises in the Okinawa Trough part 3: crustal structure of the southern Okinawa Trough. Bull Earthquake Res Inst Univ Tokyo 66: 37–70
Hoang NT, Flower MFJ (1998) Petrogenesis of Cenozoic basalts from Vietnam: implication for origins of a ''diffuse igneous province''. J Petrol 39: 34–50
Hochstaedter AG, Kepezhinskas P, Defant M (1996) Insights into the volcanic arc mantle wedge from magnesian lavas from the Kamchatka arc. J Geophys Res 101: 697–712
Ishihara K, Yoshida A (1992) Configuration of the Philippine Sea slab and seismic activity in and around Kyushu. J Seismol Soc Jpn 45: 45–51
Isozaki Y (1996) Anatomy and genesis of a subduction-related orogen: a new view of geotectonic subdivision and evolution of the Japanese islands. Island Arc 5: 289–320
Isozaki Y, Nishimura Y (1989) Fusaki Formation, Jurassic subduction–accretion complex on Ishigaki Island, southern Ryukyus, and its geologic implication to late Mesozoic convergent margin of East Asia. Mem Geol Soc Jpn 33: 259–275
Iwasaki T, Hirata N, Kanazawa T, Melles J, Suyehiro K, Urabe T, Möller L, Makris J, Shimamura H (1990) Crustal and upper mantle structure in the Ryukyu Island Arc deduced from deep seismic sounding. Geophys J Int 102: 631–651
Joshima M, Shibata K, Ono K, Ujike O (1978) Paleomagnetism and K–Ar age of the volcanic rocks from Kuro-shima island, Kagoshima prefecture. Rock Magnet Paleogeophys Research Group Japan, Annual Progress Report of the Rock Magnetism and Paleogeophysics Research Group in Japan, vol 5, pp 65–68
Kamata H, Kodama K (1994) Tectonics of an arc-arc junction: an example from Kyushu Island at the junction of the southwestern Japan Arc and the Ryukyu Arc. Tectonophysics 233: 69–81
Kao H, Chen W-P (1991) Earthquakes along the Ryukyu-Kyushu arc: Strain segmentation, lateral compression, and the thermomechanical state of the plate interface. J Geophys Res 96: 21443–21485
Keppler H (1996) Constraints from partitioning experiments on the composition of subduction-zone fluids. Nature 380: 237–240
Kersting AB, Arculus RJ, Gust DA (1996) Lithospheric contributions to arc magmatism: Isotope variations along strike in volcanoes of Honshu, Japan. Science 272: 1464–1467
Kizaki K (1986) Geology and tectonics of the Ryukyu Islands. Tectonophysics 125: 193–207
Kodaira S, Iwasaki T, Urabe T, Kanazawa T, Egloff F, Makris J, Shimamura H (1996) Crustal structure across the middle Ryukyu trench obtained from ocean bottom seismographic data. Tectonophysics 263: 39–60
Kodama K, Nakayama K (1993) Paleomagnetic evidence for post-late Miocene intra-arc rotation of south Kyushu, Japan. Tectonics 12: 35–47
Kodama K, Tashiro H, Takeuchi T (1995) Quaternary counter-clockwise rotation of south Kyushu, southwest Japan. Geology 23: 823–826
Kogiso T, Tatsumi Y, Nakano S (1997) Trace element transport during dehydration processes in the subducted oceanic crust: 1. Experiments and implications for the origin of ocean island basalts. Earth Planet Sci Lett 148: 193–206
Konishi K, Tsuji Y, Goto T, Tanaka T (1978) Holocene raised reef drilling at Kikai-jima, central Ryukyus. Sci Rep Kanazawa Univ 23: 129–153
Kurasawa H (1968) Isotopic composition of lead and concentrations of uranium, thorium, and lead in volcanic rocks from Dogo of the Oki Islands, Japan. Geochem J 2: 11–28
Le Maitre RW, Bateman P, Dudek A, Keller J, Lameyre Le Bas MJ, Sabine PA, Schmid R, Sorensen H, Streckeisen A, Woolley AR, Zanettin B (1989) A classification of igneous rocks and glossary of terms. Blackwell, Oxford
Letouzey J, Kimura M (1986) The Okinawa Trough: genesis of a back-arc basin developing along a continental margin. Tectonophysics 125: 209–230
MacDonald GA, Katsura T (1964) Chemical composition of Hawaiian lavas. J Petrol 5: 83–133
McCulloch MT, Gamble JA (1991) Geochemical and geodynamical constraints on subduction zone magmatism. Earth Planet Sci Lett 102: 358–374
Miyazaki S, Tsuji H, Hatanaka Y (1996) Velocity of horizontal crustal deformation in Japan observed by GPS: Part 2 (abstract). Jpn Earth Planet Sci Joint Meeting, Tokyo, p 646
Montagner JP, Tanimoto T (1991) Global upper mantle tomography of seismic velocities and anisotropies. J Geophys Res 96: 20,337–20,351
Mukasa SB, McCabe R, Gill JB (1987) Pb-isotopic compositions of volcanic rocks in the West and East Philippine island arcs: presence of the Dupal isotopic anomaly. Earth Planet Sci Lett 84: 153–164
Nagamune T (1987) Intermediate-depth earthquakes and tectonics of the Kyushu-Ryukyu region. J Seismol Soc Jpn 40: 417–423
Nagao T, Hase Y, Ikawa T, Nagamine S, Sakaguchi K, Yamamoto M, Shuto K, Hayashida K (1995) Characteristics of andesites forming lava plateaus in Kyushu, SW Japan: proposal of ''flood andesite''. Mem Geol Soc Jpn 44: 155–164
Nagao T, Hase Y, Nagamine S, Kakubuchi S, Sakaguchi K (1999) Late Miocene to middle Pleistocene Hisatsu volcanic rocks generated from heterogeneous magma sources: evidence from temporal-spatial variation of distribution and chemistry of the rocks. J Jpn Assoc Mineral Petrol Econ Geol 94: 461–481
Nakada S (1986) Comparative study of chemistry of rocks from the Kirishima, and the Daisen volcanic belts in Kyushu, southwest Japan. Bull Volcanol Soc Jpn 31: 95–110
Nakada S, Kamata H (1991) Temporal change in chemistry of magma source under Central Kyushu, southwest Japan: progressive contamination of mantle wedge. Bull Volcanol 53: 182–194
Nakamura E, Campbell IH, Sun S-S (1985) The influence of subduction processes on the geochemistry of Japanese alkaline basalts. Nature 316: 55–58
Nakamura E, McCulloch MT, Campbell IH (1990) Chemical geodynamics in the back-arc region of Japan based on the trace element and Sr–Nd isotopic compositions. Tectonophysics 174: 207–233
Notsu K, Arakawa Y, Kobayashi T (1990) Strontium isotopic characteristics of arc volcanic rocks at the initial stage of subduction in western Japan. J Volcanol Geotherm Res 40: 181–196

Pearce JA, Peate DW (1995) Tectonic implications of the composition of volcanic arc magmas. Ann Rev Earth Planet Sci 23: 251–285
Peng ZC, Zartman RE, Futa K, Chen DG (1986) Pb-, Sr- and Nd-isotopic systematics and chemical characteristics of Cenozoic basalts, eastern China. Chem Geol 59: 3–33
Plank T, Langmuir CH (1993) Tracing trace elements from sediment input to volcanic output at subduction zones. Nature 362: 739–743
Plank T, Langmuir CH (1998) The chemical composition of subducting sediment and its consequences for the crust and mantle. Chem Geol 145: 325–394
Seno T (1999) Syntheses of the regional stress fields of the Japanese islands. Island Arc 8: 66–79
Seno T, Stein S, Gripp AE (1993) A model for the motion of the Philippine Sea Plate consistent with NUVEL-1 and geological data. J Geophys Res 98: 17941–17948
Shimoda G, Nohda S (1995) Lead isotope analyses: an application to GSJ standard rock samples, vol 4. Human Environmental Studies, Kyoto University, pp 29–36
Shimoizumi M, Mogi T, Nakada M, Yukutake T, Handa S, Tanaka Y, Utada H (1997) Electrical conductivity anomalies beneath the western sea of Kyushu, Japan. Geophys Res Lett 24: 1551–1554
Shinjo R, Chung S-L, Kato Y, Kimura M (1999) Geochemical and Sr–Nd isotopic characteristics of volcanic rocks from the Okinawa Trough and Ryukyu Arc: implications for the evolution of a young, intracontinental back arc basin. J Geophys Res 104: 10591–10608
Shiono K, Mikumo T, Ishikawa Y (1980) Tectonics of the Kyushu–Ryukyu arc as evidenced from seismicity and focal mechanism of shallow to intermediate-depth earthquakes. J Phys Earth 28: 17–43
Sibuet J-C Letouzey J, Barbier F, Charvet J, Foucher J-P, Hilde TWC, Kimura M, Ling-Yun C, Marsset B, Muller C, Stéphan J-F (1987) Back arc extension in the Okinawa Trough. J Geophys Res 92: 14041–14063
Sibuet J-C, Hsu S-K, Shyu C-T, Liu C-S (1995) Structural and kinematic evolutions of the Okinawa Trough backarc basin. In: Taylor B (ed) Backarc basins: tectonics and magmatism. Plenum Press, New York, pp 343–379
Sibuet J-C, Deffontaines B, Hsu S-K, Thareau N, Le Formal J-P, Liu C-S, ACT party (1998) Okinawa trough backarc basin: early tectonic and magmatic evolution. J Geophys Res 103: 30245–30267
Smith AD (1998) The geodynamic significance of the DUPAL anomaly in Asia. In: Flower MFJ, Chung S-L, Lo C-H, Lee T-Y (eds) Mantle dynamics and plate interactions in East Asia. Am Geophys Union Geodynamics 27: 89–105
Stolper E, Newman S (1994) The role of water in the petrogenesis of Mariana trough magmas. Earth Planet Sci Lett 121: 293–326
Sun S-S (1980) Lead isotopic study of young volcanic rocks from mid-ocean ridges, ocean islands and island arcs. Philos Trans R Soc Lond A297: 409–445
Sun S-S, McDonough WF (1989) Chemical and isotopic systematics of oceanic basalts: implications for mantle composition and processes. In: Saunders AD, Norry MJ (eds) Magmatism in the ocean basins. Geol Soc Lond Spec Pub 42: 313–345
Tada T (1985) Spreading of the Okinawa Trough and its relation to the crustal deformation in Kyushu (2). J Seismol Soc Jpn 38: 1–12
Tatsumi Y, Tsunakawa H (1992) Cenozoic volcanism, stress gradient and back-arc opening in the North Island, New Zealand: origin of Taupo–Rotorua depression. Island Arc 1: 40–50
Tatsumi Y, Hamilton DL, Nesbitt RW (1986) Chemical characteristics of the fluid phase released from a subducted lithosphere and the origin of arc magmas: evidence from high pressure experiments and natural rocks. J Volcanol Geotherm Res 29: 293–309
Tatsumoto M, Nakamura Y (1991) DUPAL anomaly in the Sea of Japan: Pb, Nd and Sr isotopic variations at the eastern Eurasian continental margin. Geochim Cosmochim Acta 55: 3697–3708
Tatsumoto M, Basu AR, Wankang H, Junwen W, Guanghong X (1992) Sr, Nd, and Pb isotopes of ultramafic xenoliths in volcanic rocks of eastern China: enriched components EM I and EM II in subcontinental lithosphere. Earth Planet Sci Lett 113: 107–128
Taylor SR, McLennan SM (1985) The continental crust: its composition and evolution. Blackwell, Oxford
Terakado Y, Shimizu H, Masuda A (1988) Nd and Sr isotopic variations in acidic rocks formed under a peculiar tectonic environment in Miocene southwest Japan. Contrib Mineral Petrol 99: 1–10
Terakado Y, Fujitani T, Walker RJ (1997) Nd and Sr isotopic constraints on the origin of igneous rocks resulting from the opening of the Japan Sea, southwestern Japan. Contrib Mineral Petrol 129: 75–86
Tiba T (1989) Petrochemistry of the volcanic rocks from Kuchinoshima, Nakano-shima and Suwanose-jima, Tokara Islands. Mem Nat Sci Mus Tokyo 22: 7–19
Tokuyama H, Kong YS, Nasu N (1985) Collision of the Amami Plateau with the Ryukyu Island Arc. In: Nasu N, Kobayashi K, Uyeda S, Kushiro I, Kagami H (ed) Formation of active ocean margins. Terra Sci Pub, Tokyo, pp 853–873
Tsukui M, Aramaki S (1990) The magma reservoir of the Aira pyroclastic eruption – a remarkably homogeneous high-silica rhyolite magma reservoir. Bull Volcanol Soc Jpn 35: 231–248
Tu K, Flower MFJ, Carlson RW, Xie G, Chen C-Y, Zhang M (1992) Magmatism in the South China Basin, 1. Isotopic and trace-element evidence for an endogenous Dupal mantle component. Chem Geol 97: 47–63
Turner S, McDermott F, Hawkesworth C, Kepezhinskas P (1998) A U-series study of lavas from Kamchatka and the Aleutians: constraints on source composition and melting processes. Contrib Mineral Petrol 133: 217–234
Uto K, Uchiumi S (1997) K–Ar ages for Maruyama lava domes in Hiwaki town, Kagoshima Prefecture, southwest Japan: a Quaternary volcano constituting a second volcanic row of Ryukyu arc. Bull Volcanol Soc Jpn 42: 299–302
Uto K, Sakaguchi K, Teraoka Y, Okumura K, Komazawa M (1997) Geological map of Japan 1: 200,000, Kagoshima. Geol Surv Jpn
Wallace PJ, Carmichael ISE (1999) Quaternary volcanism near the Valley of Mexico: implications for subduction zone magmatism and the effects of crustal thickness variations on primitive magma compositions. Contrib Mineral Petrol 135: 291–314
Watanabe K, Izawa E, Kiyoura T, Sekine R, Itaya T, Danhara T (1993) Time and space change of Neogene volcanism in Kyushu (abstract). Geol Soc Japan Meeting, Tokyo, p 289
Woodhead JD, Volker F, McCulloch MT (1995) Routine lead isotope determinations using a lead-207–lead-204 double spike: a long-term assessment of analytical precision and accuracy. Analyst 120: 35–39
Yamamoto H (1993) Submarine geology and post-opening tectonic movements in the southern region of the Sea of Japan. Mar Geol 112: 133–15